4. 3-D NUMERICAL ANALYSIS OF GROUNDED ELECTRIC DIPOLE SOURCE TRANSIENT ELECTROMAGNETIC METHOD

4.1 INTRODUCTION

It is well known that conventional inductive EM methods do not provide accurate images of thin resistors compared to those of thin conductors (Hordt et al., 2002). In contrast to conventional inductive EM methods, the GESTEM method can generate vertical transient currents as well as horizontal transient currents, and therefore will be better able to detect a thin resistor at depth. While the previous work (Gunderson et al., 1986 and Newman, 1989) concerning a grounded electric source mostly focused on broadside vertical magnetic field measurements and explanations of the governing physics, the work done here provides more comprehensive modeling results for various grounded electric source – receiver configurations.

4.2 NUMERICAL MODELING METHODS

To investigate how transient EM fields of the GESTEM method diffuse and how they are different from those of the standard loop TEM method, the step-off EM responses of the two EM methods were calculated for three different one-dimensional models: a background model, a resistor model, and a conductor model (Figure 4.1). The layered earth model code, EM1DSheet from Lawrence Berkeley Laboratory was used for these computations. Even though EM receivers can only be placed on the earth's surface in practice or limited number of boreholes, a number of imaginary EM receivers were

employed within the earth along cross-sections of the models of interest. This methodology allows us to analyze how the transient fields diffuse below the surface with time and how they interact with target layers. Thus, the physics of the EM methods can be directly observed.

The 250 m long GESTEM source was placed on the earth's surface. The loop TEM method employs a 250 m *250 m square source loop for a consistent comparison to the GESTEM response. The ramp-off time for the two methods is set to 1.0E-4 seconds. The driving current is set to 40 A. The electric receiver noise level is set to $1.0E^{-10}$ (V/m) and the magnetic receiver noise level to $1.26E^{-5}$ (nT) (Ed Nichols, personal communication).

The GESTEM survey geometry can be defined in terms of the source-receiver azimuth, i.e. the angle between the source dipole axis and the line joining the source and receiver. At an azimuth of 90 degrees (broadside configuration), an inductive response dominates. In the orthogonal direction at an azimuth of 0 degrees (in-line configuration), both galvanic and inductive responses are effective. Strong dependence of the response on source-receiver geometry will be exemplified in this numerical modeling study. As for the AMT method, the source frequencies from $1.0E^{-3}$ Hz to $1.0E^{5}$ Hz were employed to generate an apparent resistivity sounding curve and impedance phase curve.

4.3 NUMERICAL MODELING RESULTS

4.3.1 HOMOGENEOUS HALF SPACE MODEL

In order to compare the physics of the Loop TEM method to that of the in-line GESTEM method, the successive snapshots of transient current distribution in the background model are plotted in Figure 4.2 for the Loop TEM method and Figure 4.3 for the in-line GESTEM method. Nabighian (1979) described the time domain induced current system shown in Figure 4.2 as resembling a "smoke ring" blown by the transmitter. In the homogeneous background model, the current maximum of the Loop TEM method moves outward and downward from the loop source edge at an angle of approximately 30 degrees with the surface. As is known well, this induced current system consists of only horizontal currents. In contrast to the Loop TEM method, the in-line GESTEM method can generate both horizontal and vertical transient current fields. Therefore, the induced current system of the in-line GESTEM method can be examined effectively with three types of plots as shown in Figure 4.3: total current plots; horizontal current plots; and vertical current plots. To supplement Figure 4.3, the 3-D snapshots of current density are shown in Figure 4.4.

The horizontal currents with the in-line GESTEM source consist of two parts. The upper horizontal current system, 'the image of the source' diffuses equally in the x- and y-directions, but the locus of its maximum remains very close to the source over the whole measurement time. The lower horizontal current system, the so-called 'return current'

(Gunderson et al, 1986), diffuses downward relatively quickly but has a much smaller amplitude than the upper currents. As the horizontal current maximum remains close to the source over the time, the magnetic and electric responses of the GESTEM method have a static shift problem if there is an inhomogeneity near the source (Newman, 1989).

The vertical current system shows important aspects. First, the vertical current maximum diffuses rapidly in depth, but its amplitude decays as slowly as the horizontal current maximum decays over time. This rapid-depth-diffusion is illustrated by plotting locus of the current maximum at each measurement time (Figure 4.5), while the amplitude of the current maximum as a function of time, and the amplitude of current maximum as a function of depth, are plotted in Figure 4.6a and Figure 4.6b respectively. Notice that the total current maximum of the GESTEM method is not the sum of vertical current maximum and horizontal current maximum because they exist at different locations. Hence, the locus of the GESTEM total current maximum is the same as the locus of the horizontal current maximum. At a given time, the amplitude of the GESTEM vertical current maximum is about 30% of that of the GESTEM horizontal current maximum as shown in Figure 4.6a, but, at a given depth, the amplitude of the GESTEM vertical current maximum is always larger than the other components. Thus, Figure 4.6 implies that the responses due to this fast diffusing and highly concentrated vertical current can sense a target in depth at earlier time than other components. This characteristic will be illustrated in section 4.3.3.

Second, the diffusion angle of the vertical current maximum is about 45 degrees from the source edge on the surface as observed in Figure 4.3 and Figure 4.5. That is, the vertical current for the GESTEM method is more focused below the source than the horizontal current for the Loop TEM method.

Third, the GESTEM vertical current maximum and most of the GESTEM vertical currents stay on, or in the vicinity of the plane, which contains the source (Figure 4.4) while the GESTEM horizontal currents diffuse evenly in the x- and y- directions.

Unlike the in-line GESTEM method, the standard LOTEM method (vertical magnetic field measurement using the broadside GESTEM method) utilizes the time-derivative of the transient vertical magnetic field. The snapshots of transient currents in the background model are plotted in Figure 4.7 for the broadside LOTEM method. Notice that there are only horizontal currents along the broadside cross-section. Therefore, the measured magnetic responses for the LOTEM method are mainly inductive arising from horizontal current flow.

Lastly, the induced current field for the AMT method at 100 Hz is presented in Figure 4.8. Notice that there are only horizontal induced currents in the earth and their amplitudes decrease as the depth increases.

4.3.2 1-D RESISTOR MODEL

The primary reason to use the GESTEM method over others is to delineate the geometry of thin resistive bodies in depth. This section provides the 1-D numerical modeling examples that demonstrate how the Loop TEM method and the AMT method fail to sense a thin resistive layer shown in Figure 4.1b, while the GESTEM method detects it.

The Loop TEM responses are shown for different receiver locations in Figure 4.9. There is no distinguishable difference between the 1-D resistor model and the background model. The cause of the identical response is verified by viewing the difference between transient current distribution for the 1-D resistor model (Figure 4.10) and the background model (Figure 4.2). The locus of current maximum for the two models is in similar positions at each time and the overall patterns of the current distribution for the two models are also similar in space.

For easier analysis, the locus of the current maximum at each measurement time is plotted in Figure 4.11, which can be compared to Figure 4.5. The standard loop TEM system measures vertical magnetic fields which entirely originate from horizontal current flows in the earth. The similar horizontal current distributions in the two models at each time induce similar magnetic field response on the surface. As a result, the magnetic field measurements of the loop TEM method fails to detect a thin resistor in depth.

The in-line GESTEM responses are computed and shown for a few different receiver locations in Figure 4.12 for dB_Y/dt measurements, and in Figure 4.13 for E_X measurements. While the dB_Y/dt measurements for the 1-D resistor model are identical to those for the background model, the E_X measurements show small differences between the two models. The nearly identical magnetic field response results are explained by the small differences noted when comparing the horizontal current field distribution for the background model (Figure 4.3) to that for the 1-D resistor models (Figure 4.14). However, the vertical current system shows differences between the two models. As indicated in Figure 4.11 and Figure 4.14, the vertical current maximum of the 1-D resistor model moves downward quickly, develops along the upper boundary of the thin resistor, and diffuses rapidly from the center of the model. In contrast, the vertical current maximum of the background model (Figure 4.3 and Figure 4.5a) just diffuses at 45 degrees. The vertical current interacts with the 1-D resistor over time, resulting in charge buildup along the boundary of the horizontal reservoir in order to satisfy the continuity of normal current. The electric fields from these extra charges distort the geometry of the transient electric field, providing the grounded electric field receivers with the small perturbation as shown in Figure 4.13. In addition to the electric field response at a few receiver locations, 2-D snapshots of transient electric field in the 1-D resistor model are plotted in Figure 4.15. The interaction of the transient vertical currents with the resistor results in strong electric fields both in and around the resistor.

As shown in Figure 4.13, the degree of E_X perturbation due to the 1-D resistor varies as the source-receiver separation increases. In order to highlight the degree of the perturbation as the function of source-receiver separation, the 1-D resistor response was normalized by the background response at each receiver location in Figure 4.16. As source-receiver separation increases, the difference of the step-off response between the two models decreases. This is because large source-receiver separation is sensitive to the electrical properties of a much larger volume of the subsurface. Notice that the relatively large differences at a larger separation in early time are due to a time-delayed direct current (DC) response, and do not represent the electromagnetic sensing ability of the GESTEM method.

Based on Figure 4.13, the electric field measurements of the GESTEM method are able to sense a thin resistor in depth, but the difference between the two models is still small and the DC effect dominates the transient electromagnetic response coming from the thin resistor. A way to eliminate the flat (zero-slope) DC responses in Figure 4.13 and Figure 4.16 is to take the time-derivative of E_X responses. These calculations are shown in Figure 4.17. Even though taking the time-derivative results in numerical noise at early times, this mathematical manipulation clearly enhances the response coming from the thin resistor at larger separation. For smaller source-receiver separation, the difference of the time-derivative between the background and resistor models is less but the shapes is sharper. For the larger separation, the difference between the twos is larger but the amplitude is smaller and broader.

A different way to think of Figure 4.17 is that the time-derivative of the response of a step-off source having short ramp-off time is an estimate of the impulse response. The major difference between the two transmitter waveforms is frequency spectrum: the step-off transient response mainly consists of low frequency signals which are unsuitable for sensing the thin resistor in this given exploration scenario while the impulse response has a broad range of frequencies in its EM spectrum including high frequency signals and thereby gives much more information about subsurface resistivity. This modeling result with the time-derivative of step-off response illustrates that it is necessary to choose and/or design a proper transient EM pulse such that the relatively high frequencies required for reservoir detection are produced.

The LOTEM method (broadside long offset GESTEM method) has been studied by many authors and it is well known that magnetic field responses from the broadside configuration are insensitive to thin resistive layers because magnetic responses purely come from horizontal current flow in earth (Hordt et al, 2000). The broadside dB_Z/dt and broadside E_X responses are plotted in Figure 4.18 and Figure 4.19 respectively. As expected, dB_Z/dt responses fail to sense the thin resistor in depth. Broadside E_X responses still detect the presence of the thin resistor but their amplitudes are 5-6 times smaller than the amplitudes of in-line E_X responses (Figure 4.13).

Lastly, the AMT sounding results over the background model, the 1-D resistor model, and the 1-D conductor model are plotted in Figure 4.20. The 1-D resistor does not produce significant perturbations in its apparent resistivity sounding result. The induced current system of the AMT method between the background model (Figure 4.8) and the 1-D resistor model (Figure 4.21) does not show any meaningful difference because the AMT method utilizes a purely inductive source. Thus, the AMT method is inappropriate for the detection of such a thin resistive layer at depth solely.

4.3.3 1-D CONDUCTOR MODEL

In this subsection, the GESTEM method is employed to sense the thin conductive layer shown in Figure 4.1c. Delineating conductive targets is not a main concern of GESTEM application because the Loop TEM method is able to detect a thin conductor with reasonable accuracy, and does not require implanting a transmitter and receivers into the ground. However, the numerical study of the 1-D conductor model is added here for the complete understanding of the GESTEM method and for its comparison to the other methods.

The Loop TEM responses are shown for a few different receiver locations in Figure 4.9. The difference of the measured magnetic field between the background model and the 1-D conductor model in Figure 4.9 can be explained by comparing the locus of the current maximum in the background model (Figure 4.2) to that in the 1-D conductor model (Figure 4.22). The current maximum in the background model diffuses outward and

downward from the loop source edge at an angle of approximately 30 degrees with the surface (Nabighian et al., 1991). In the 1-D conductor model, the current maximum quickly diffuses into the thin conductor and stays within it. This different locus of the current maximum between the two models over the measurement time produces the different magnetic responses, and enables an interpreter to detect the presence of the thin conductor. For easier analysis, the locus of the current maximum in the 1-D conductor model at each measurement time is plotted in Figure 4.23 and compared to Figure 4.5.

The in-line GESTEM responses are computed for a few different receiver locations in Figure 4.12 for dB_Y/dt measurements and in Figure 4.13 for E_X measurements. The snapshots of the in-line GESTEM current system in the 1-D conductor model are plotted in Figure 4.24. The magnetic field response of the GESTEM method senses the thin 1-D conductor in the same way as the loop TEM method does. That is, the horizontal current maximum is confined within the conductor. For completeness, the 2-D snapshots of transient electric field in the 1-D conductor model are plotted in Figure 4.25.

The E_X measurements also sense the thin conductor but give much smaller response than the other two methods investigated. Results shown in Figure 4.13 demonstrate that GESTEM E_X measurements sense both the 1-D thin resistor and the 1-D conductor equally. This is possible because the sensing ability of GESTEM E_X measurements result from the charge buildup. That is, the polarity of charge buildup on the surface of the 1-D resistor is opposite to that on the 1-D conductor. A comparison of the depth sensitivity

versus time for sensing thin conductors between the Loop TEM method and the GESTEM method is shown in Figure 4.17b and Figure 4.9b. It is clear that the GESTEM method senses the thin conductor much earlier than the Loop TEM method does. However, there is no reason to employ the GESTEM method to sense a thin conductor because the degree of its electric field perturbation is relatively small for this type of model.

A few broadside GESTEM magnetic and electric responses for the 1-D conductor model are illustrated in Figure 4.18 and Figure 4.19 respectively. The magnetic field responses distinguish between the background model and the 1-D conductor model because the current maximum is confined to the thin conductive layer as shown in Figure 4.26.

Finally, the AMT method also works to sense the thin conductor as shown in Figure 4.20. The 1-D conductor produces much larger perturbations in its apparent resistivity sounding result than the 1-D resistor. This difference can be explained by comparing the induced current system between the background model and the 1-D conductor model. This current distribution in the 1-D conductor model (Figure 4.27) is different enough compared to that in the background model (Figure 4.8).

4.3.4 EFFECT OF NEAR-SURFACE INHOMOGENEITY ON GESTEM RESPONSES

In order to investigate the effect of near-surface inhomogeneity on GESTEM sounding results, the magnetic and electric field responses were calculated at the three receiver locations for the following models shown in Figure 4.28: the center of the near-surface conductor varies from (0m, 0m, 0m), (-300m, 0m, 0m) to (-600m, 0m, 0m).

The electric field sounding results are presented in Figure 4.29 and the magnetic field sounding results in Figure 4.30. For model 1, the magnetic and electric field responses at the three receiver locations are "shifted" down in amplitude for the entire measurement time, leading to misinterpretation of electric resistivity structure of the subsurface.

Compared to the responses for model 1, the EM responses for model 2 and model 3 show varying degrees of shift at the different receiver locations. The E_X measurements at (1 km, 0 km, 0 km) and (0 km, 1 km, 0 km), and the dB_Y/dt measurements at (1 km, 0 km, 0 km) do not suffer severely from a static shift and are roughly equal to the responses for the background model. In contrast, the E_X measurements at (-1 km, 0 km, 0 km), the dB_z/dt measurements at (0 km, 1 km, 0 km) and the dB_Y/dt measurements at (-1 km, 0 km, 0 km) have severe static shift problem over the entire measurement time.

To understand the calculations presented in Figures 4.29 and 4.30, the snapshots of current distribution were plotted in Figure 4.31 for the background model, Figure 4.32 for

model 1, Figure 4.33 for model 2, and Figure 4.34 for model 3. In model 1, both the horizontal and vertical current maximums are trapped within or in the vicinity of the conductor without lateral and downward migration over the entire measurement time. Therefore, the measurements at all the receiver locations are affected by the near-surface conductor over the entire measurement time, and do not converge to the background model response even at later times. Notice that the vertical current distribution shown in Figure 4.32d is asymmetrical with respect to the center of the model. This numerical artifact is because a finite numbers of receiver positions on the cross-section can not capture the vertical current distribution perfectly, and thus the interpolation provided by the graphics package employed is subject to error' When the center of the conductor is offset to the left of the source, more current on the right side of the source (Figure 4.33 and 4.34) diffuses outward. In addition, the separation between the center of the near-surface conductor and the measurement location becomes larger. Thus, the degree of static shift is somewhat reduced.

The modeling results illustrate that the GESTEM sounding is under strong influence of near-surface inhomogeneity and the current 1-D inversion scheme for the grounded wire source can not be a robust, reliable imaging solution to process GESTEM sounding data if these types of inhomogeneities are present.

4.3.5 3-D RESISTOR MODEL

To investigate more complicated scenarios, the previous 1-D resistor is replaced by the 3-D resistive block described in Figure 4.35. For consistency reasons, all other modeling parameters for the 3-D forward modeling are the same as those for the 1-D forward modeling. Two 3-D block models are considered in this subsection: Model 4 (Figure 4.35a) has the 3-D block 500m directly below the GESTEM source; In Model 5 (Figure 4.35b), the same 3-D block is located along the diffusion path of vertical current maximum within the background model. Thus, the effect of coupling of the vertical transient currents to the 3-D block versus position can be examined.

The numerical modeling results for the two models and the background model are shown in Figure 4.36 for the magnetic field responses and in Figure 4.37 for the electric field responses. As illustrated before, the magnetic field responses do not sense the presence of the block. In contrast, the electric field measurements show the different degree of sensing ability on the block between model 4 and 5: the presence of the block is more clearly identified in model 5 than in model 4.

In order to explain the observed electric field responses, the snapshots of the transient current system are shown in Figure 4.38 for model 4 and in Figure 4.39 for model 5. Because the block is off the path the vertical current maximum took in model 4, the vertical currents have little opportunity to interact. This results in small perturbation in the measured electric fields. When the block is moved 500m to the right from the center of the

source as shown in Figure 4.35b, the vertical current can be more efficiently coupled to the 3-D block and optimize the galvanic effect.

This modeling example demonstrates that the GESTEM method is very dependent on source-receiver configuration to sense a small localized target, and that the diffusion angle of the vertical transient currents should be considered as an important survey factor in practice.

4.4 CONCLUSIONS

The GESTEM method has been investigated numerically and compared to the other two standard terrestrial EM methods in this section. The important characteristics of the GESTEM method and its transient fields are summarized below.

First, the vertical current maximum diffuses downward at 45 degrees from the edge of the source and the fast diffusing and highly concentrated vertical currents of the GESTEM method help sense a deep resistive target in early time. Making vertical transient currents coupled efficiently to a resistive target is a crucial factor to get large perturbation.

Second, the majority of the vertical currents are confined within or near to the plane which contains the source while the GESTEM horizontal currents diffuse evenly in the x- and y-directions and slowly downward over the entire measurement time.

Third, the GESTEM method can sense both thin conductive and resistive targets equally because its response relies on galvanic response. In contrast, Loop TEM and MT methods are much more sensitive to conductive targets but fail to sense thin resistive ones because they employ purely inductive sources.

Finally, this study confirms the well known modeling result by Newman (1989) that the GESTEM sounding is very sensitive to near-surface inhomogeneity and thus can not be interpreted accurately using 1-D inversion schemes if these types of inhomogeneities are present.

4.5 FIGURES

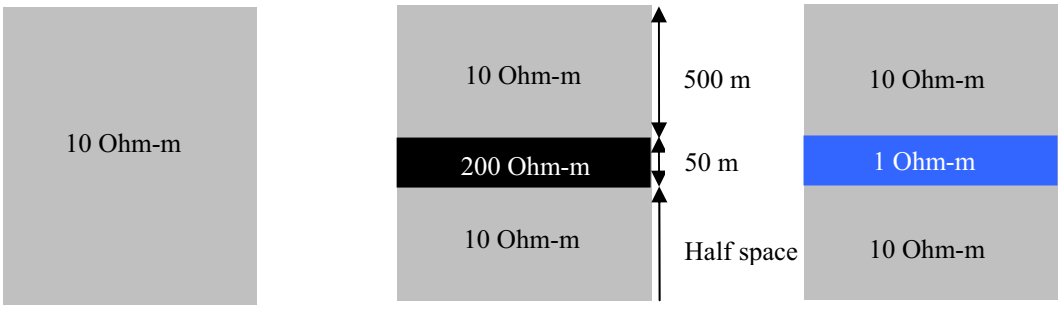

Figure 4.1. The three 1-D models: (a) background model, (b) 1-D resistor model and (c) 1-D conductor model.

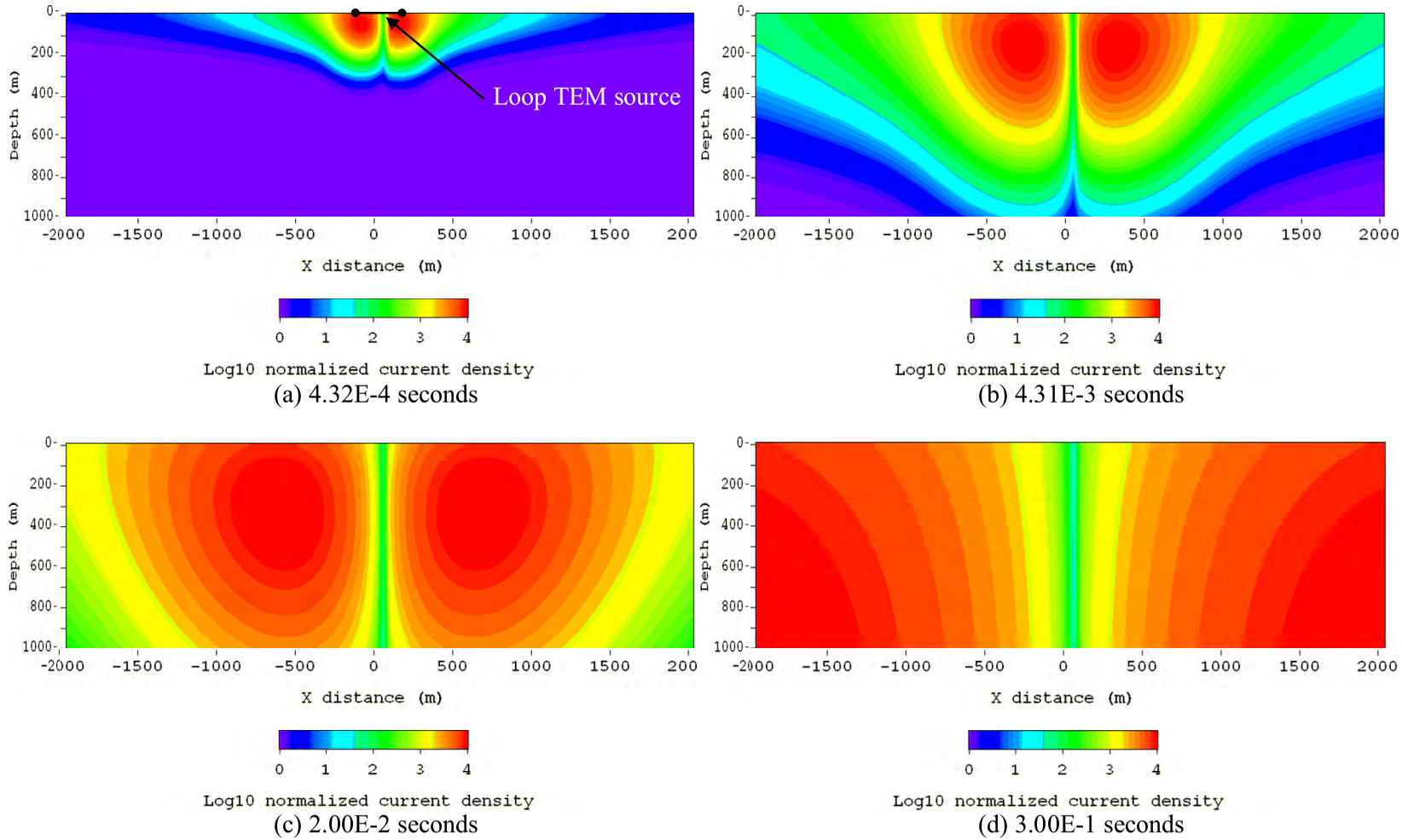

Figure 4.2. Normalized y component of the current density as a function of position in a plane bisecting 250 m *250 m loop source in the background model at the four different measurement times.

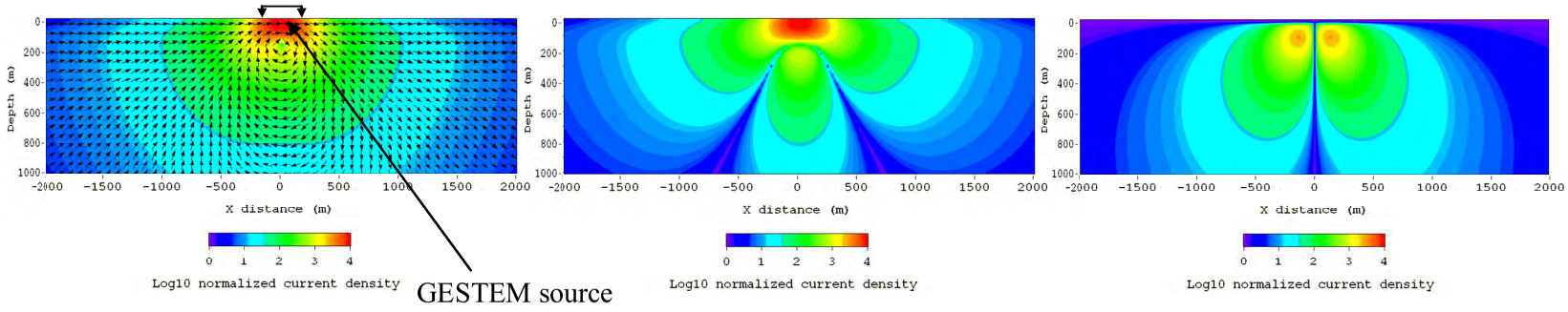

(a) 4.32E-4 seconds

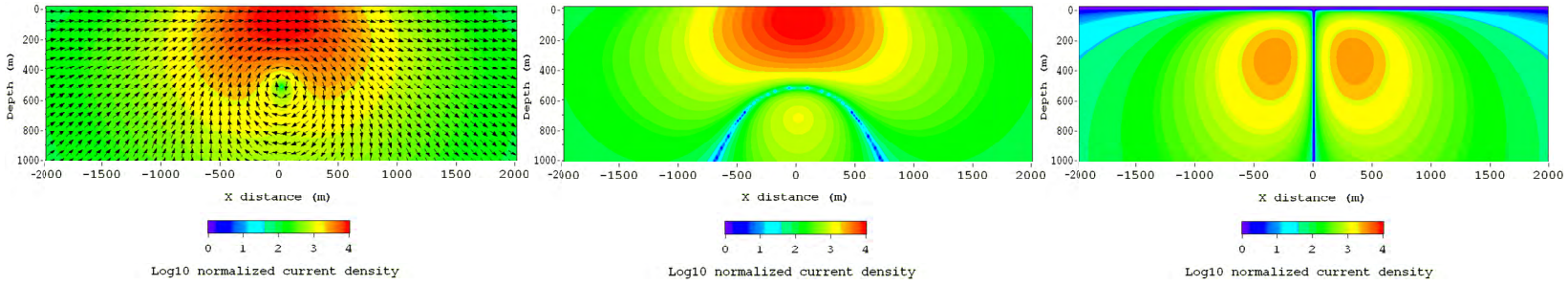

(b) 4.31E-3 seconds

Figure 4.3. Normalized current density as a function of position in the cross-section including a 250 m long grounded source in the background model at the four different measurement times. Total current density (left), horizontal current density (middle) and vertical current density (right).

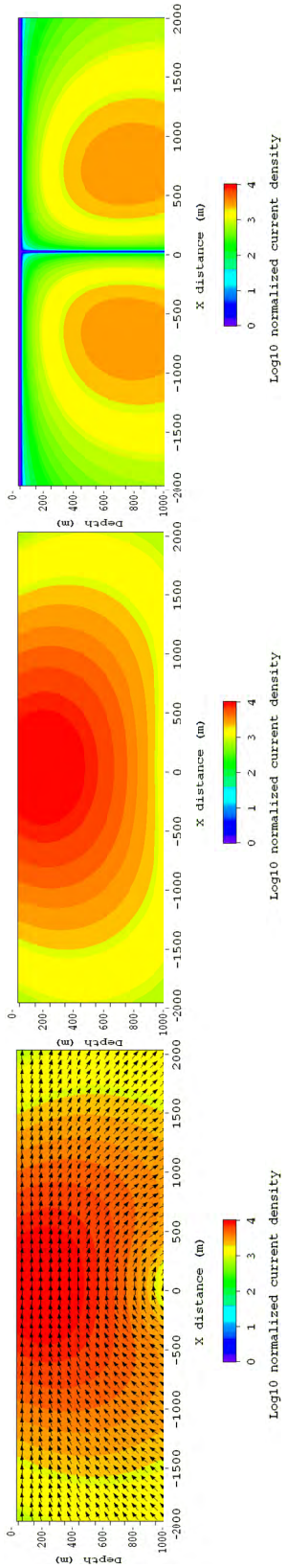

(c) 2.00E-2 seconds

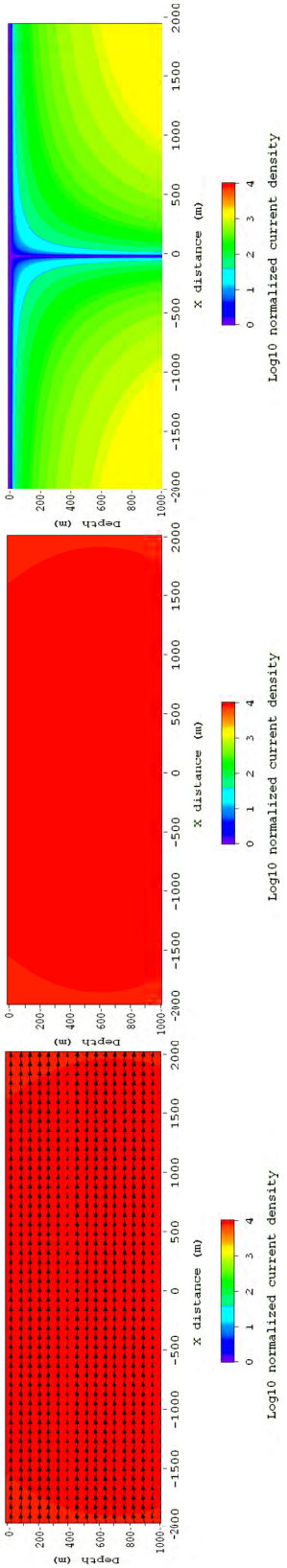

(d) 3.00E-1 seconds

Figure 4.3. Continued.

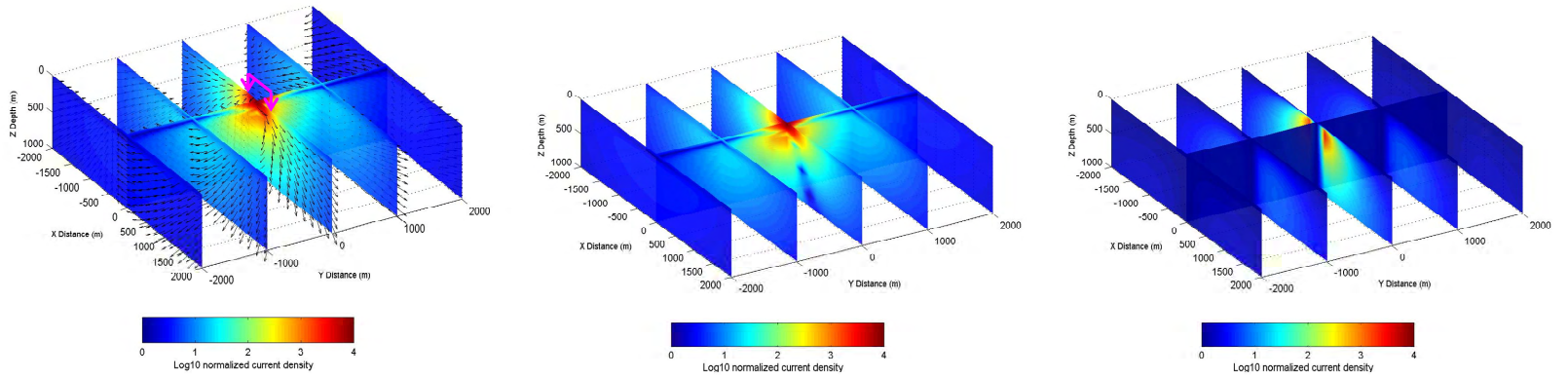

(a) 4.32E-4 seconds

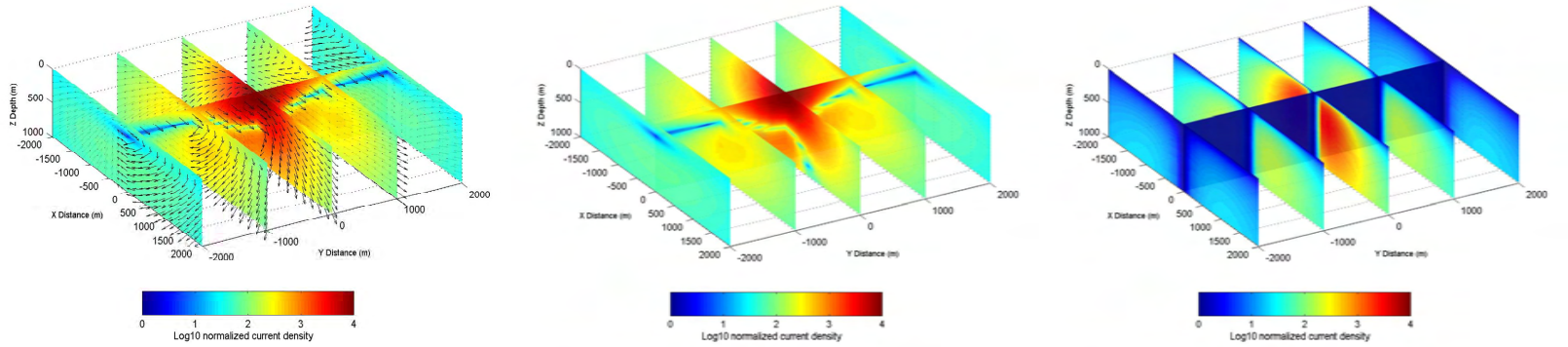

(b) 4.31E-3 seconds

Figure 4.4. 3-D normalized current density in the background model at four different measurement times. Total current density (left), horizontal current density (middle) and vertical current density (right).

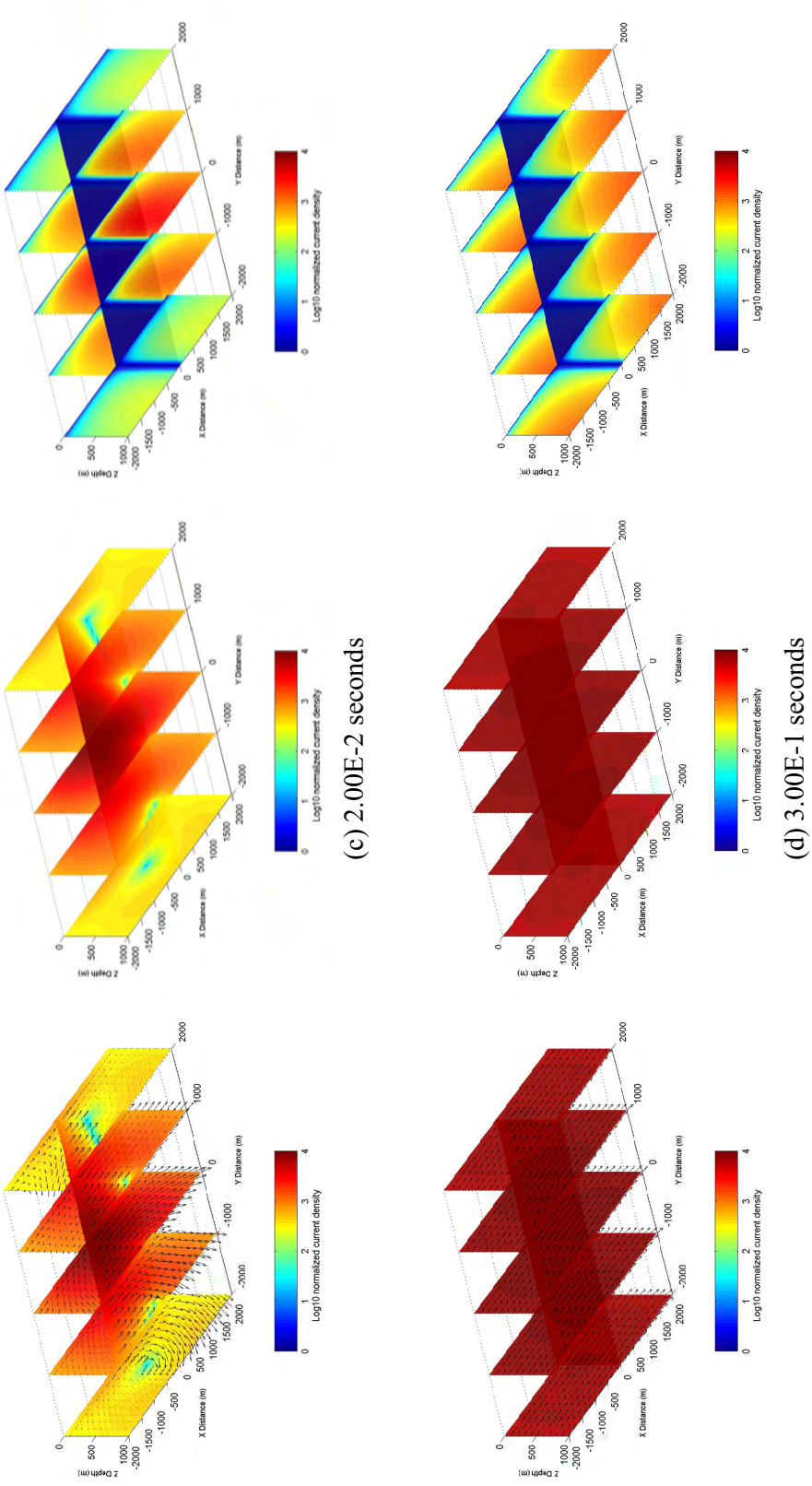

(c) 2.00E-2 seconds

(d) 3.00E-1 seconds

Figure 4.4. Continued.

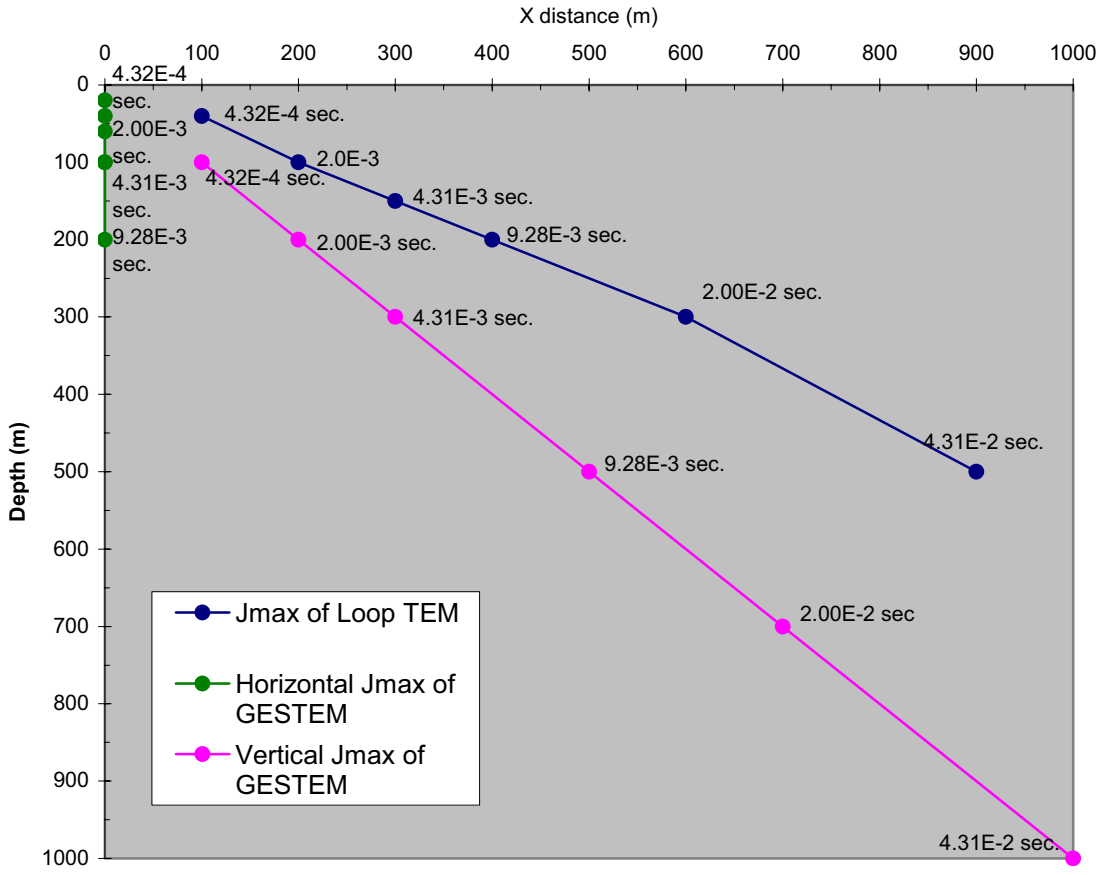

Figure 4.5. Locus of the current maximum in the background model.

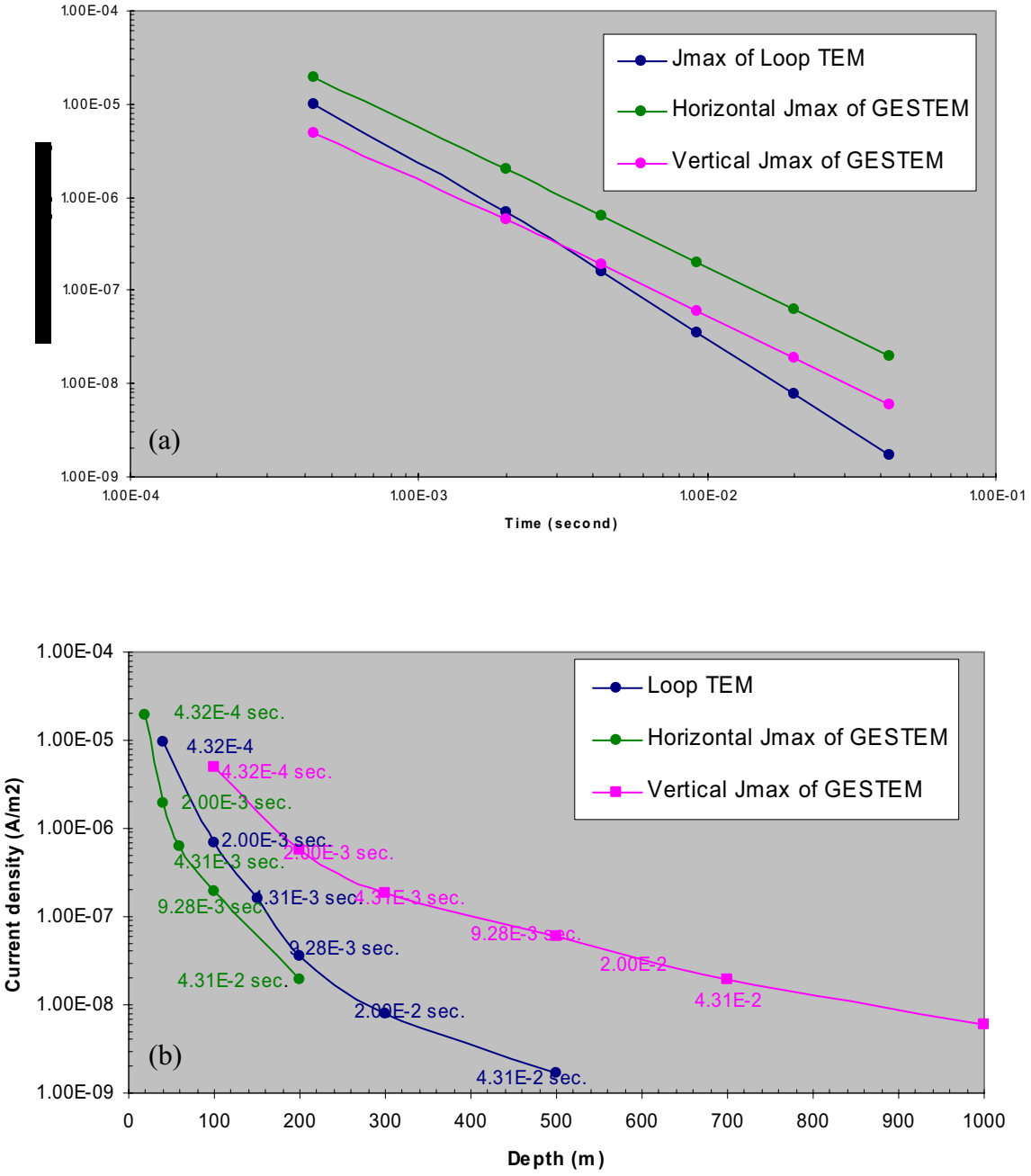

Figure 4.6. The characteristics of the current maximum for the loop TEM and the GESTEM in background model. (a) the current maximum amplitude as a function of time in the background model and (b) the current maximum amplitude as a function of depth.

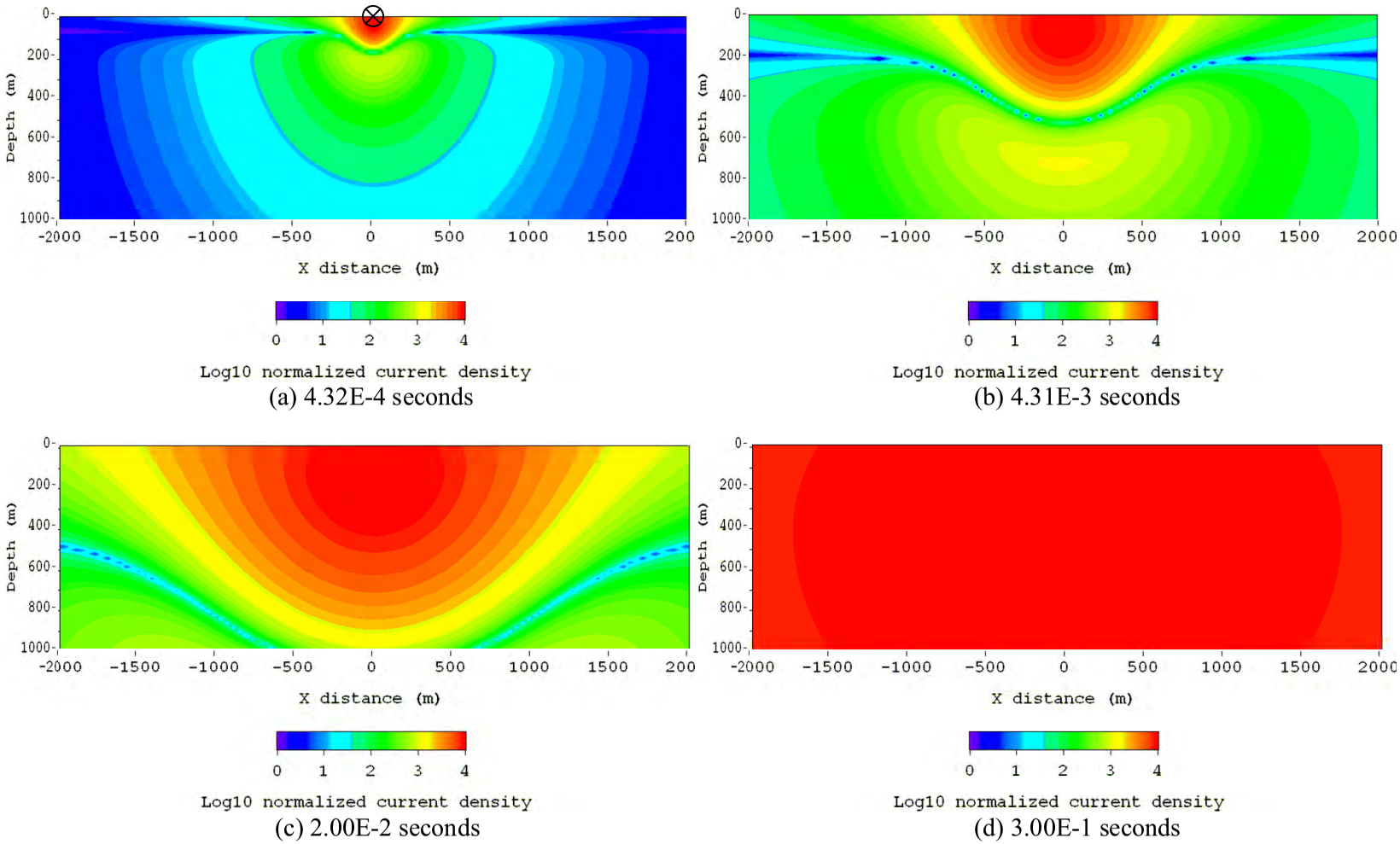

Figure 4.7. Normalized current density as a function of position in the cross-section bisecting a 250 m long grounded source in the background model at the four different measurement times. The direction of current at every position is parallel to the source orientation.

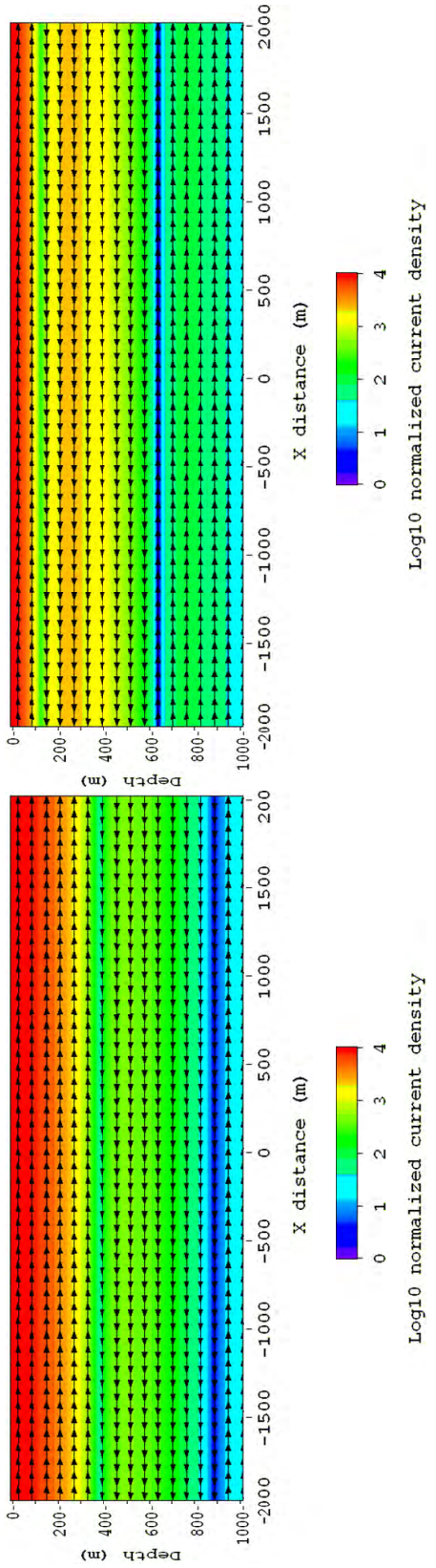

(a) In-phase

(b) Out-of-phase

Figure 4.8. Normalized in-phase and out-of-phase current density in the background model due to 100 Hz AMT plane wave source.

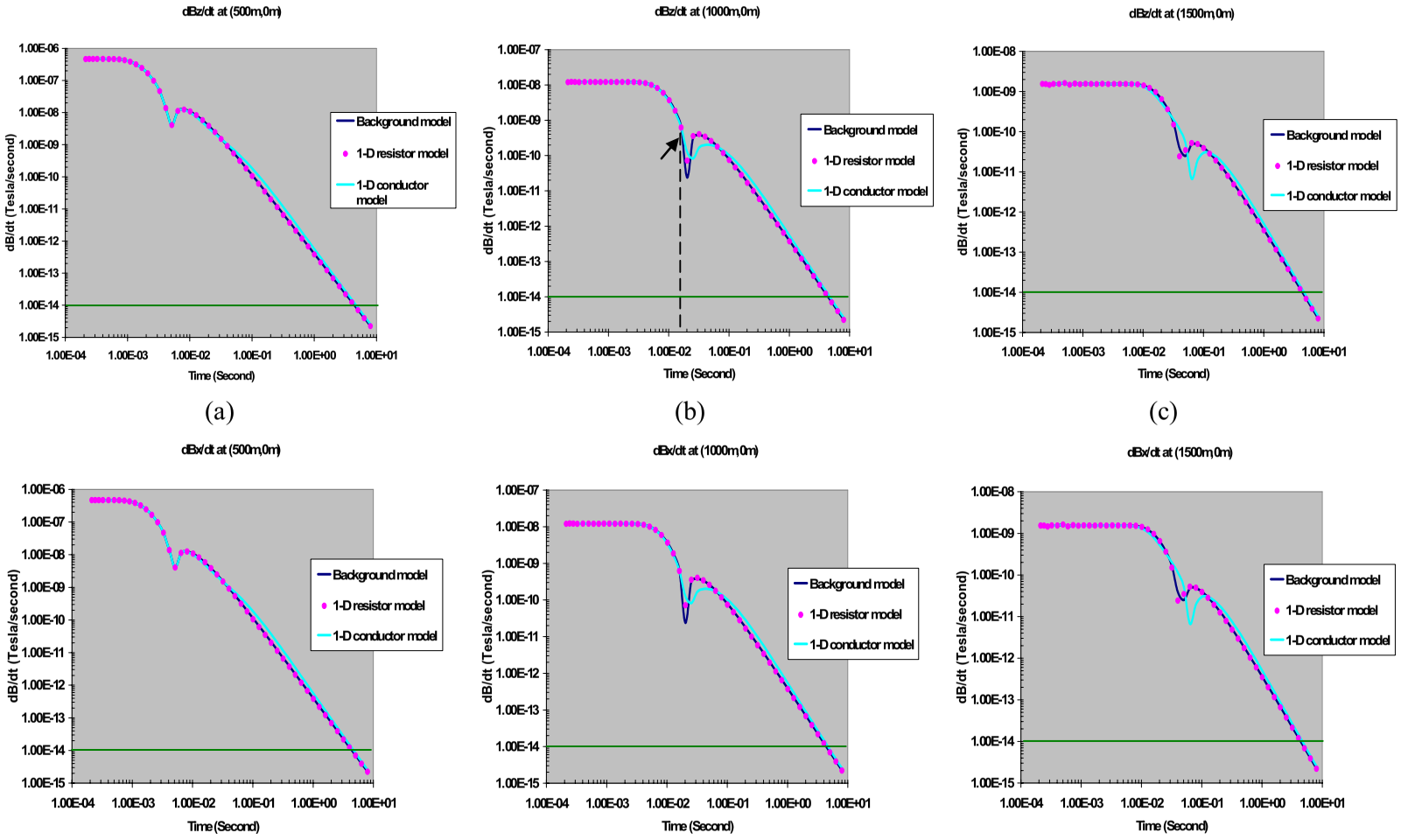

Figure 4.9. Magnetic field responses at the three different receiver locations with 250 m * 250 m loop TEM source. The arrow in the (b) represents the time when the loop TEM method first starts to sense the presence of the thin conductor. The green lines represent receiver noise level.

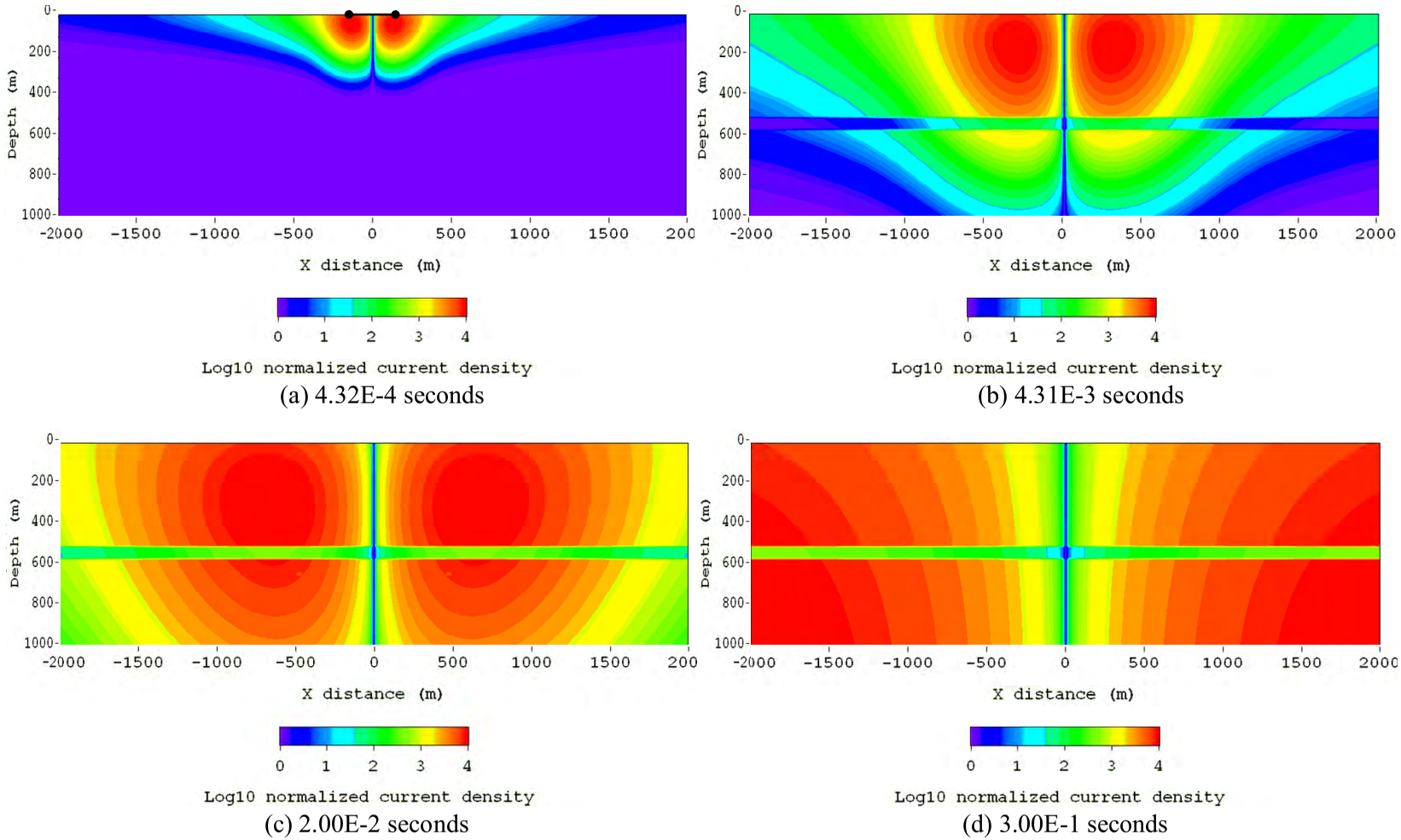

Figure 4.10. Normalized current density as a function of position in a plane bisecting a 250 m * 250 m loop source in the 1-D resistor model at the four different measurement times.

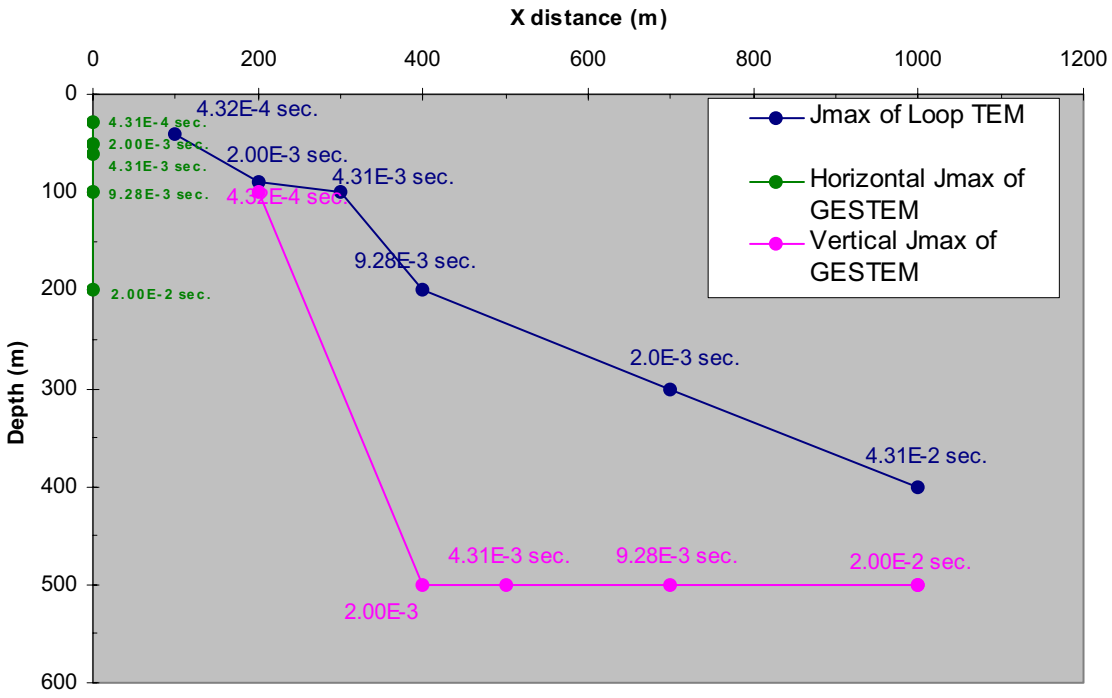

Figure 4.11. Locus of the current maximum in the 1-D resistor model for different times during the decay.

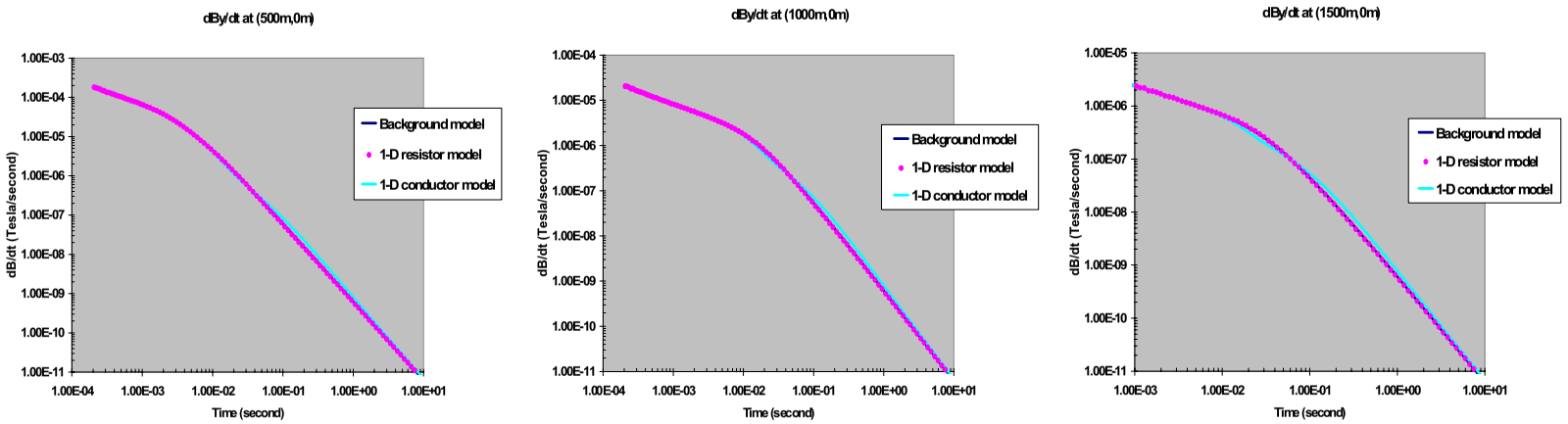

(a) (b) (c)

Figure 4.12. In-line magnetic field response at the three different receiver locations with a 250 m long grounded source.

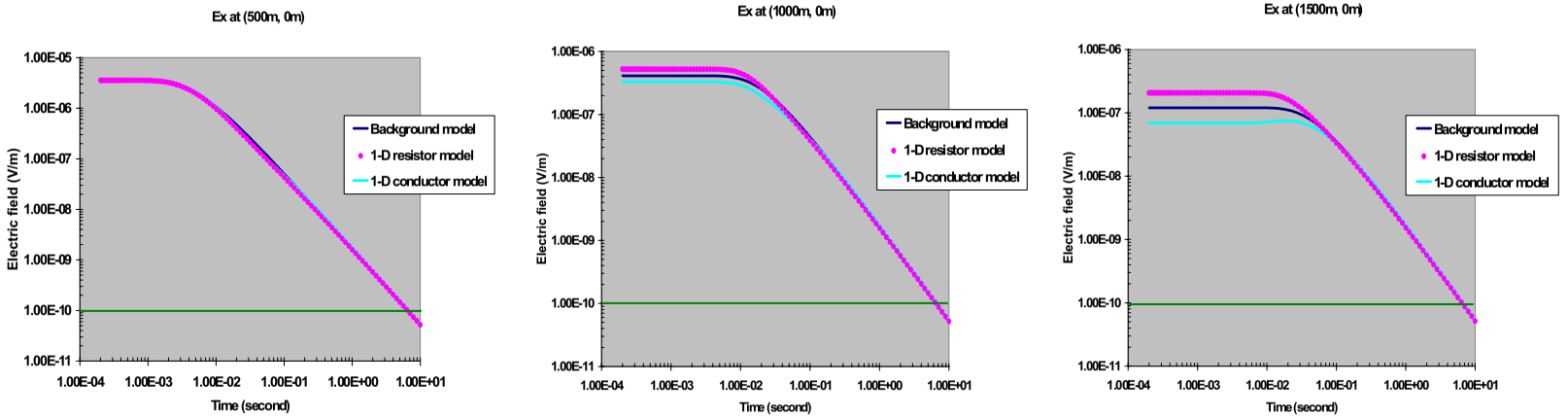

(a) (b) (c)

Figure 4.13. In-line electric field response at the three different receiver locations with a 250 m long grounded source. The green lines represents receiver noise level.

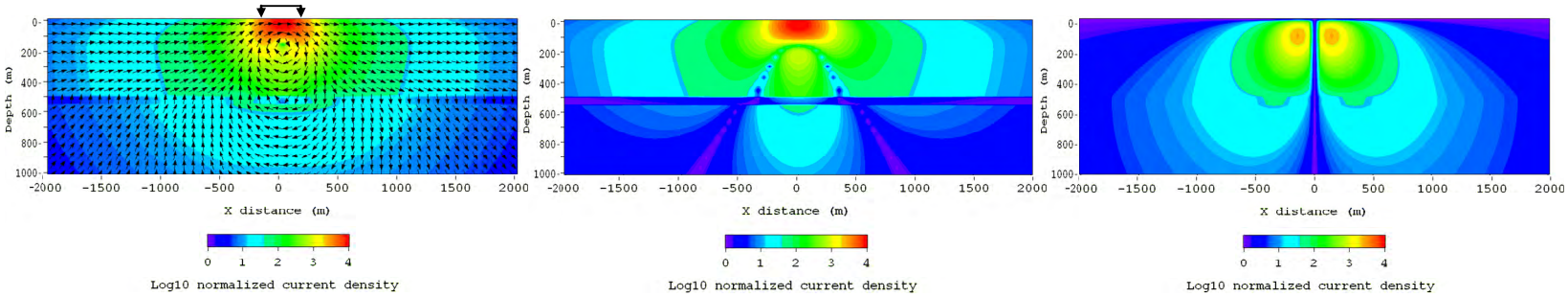

(a) 4.32E-4 seconds

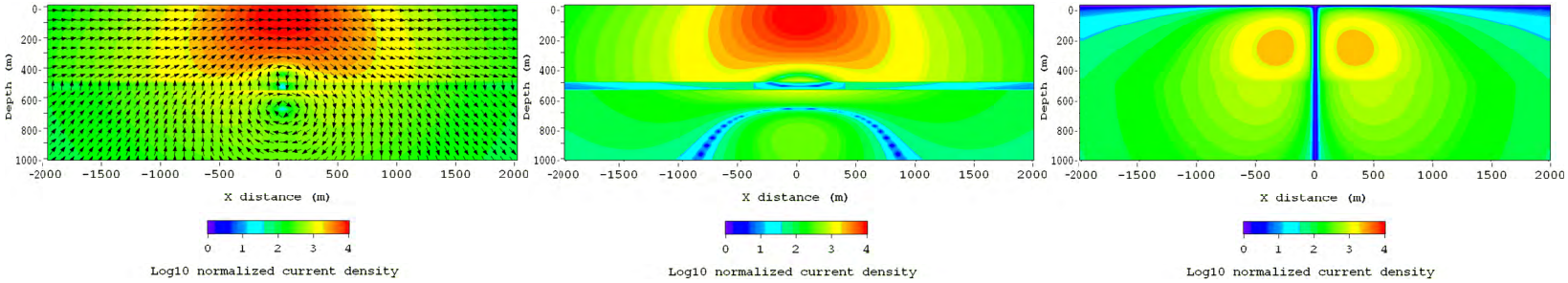

(b) 4.31E-3 seconds

Figure 4.14. Normalized current density as a function of position in the cross-section including a 250 m long grounded source for the 1-D resistor model at four different measurement times. Total current density (left), horizontal current density (middle) and vertical current density (right).

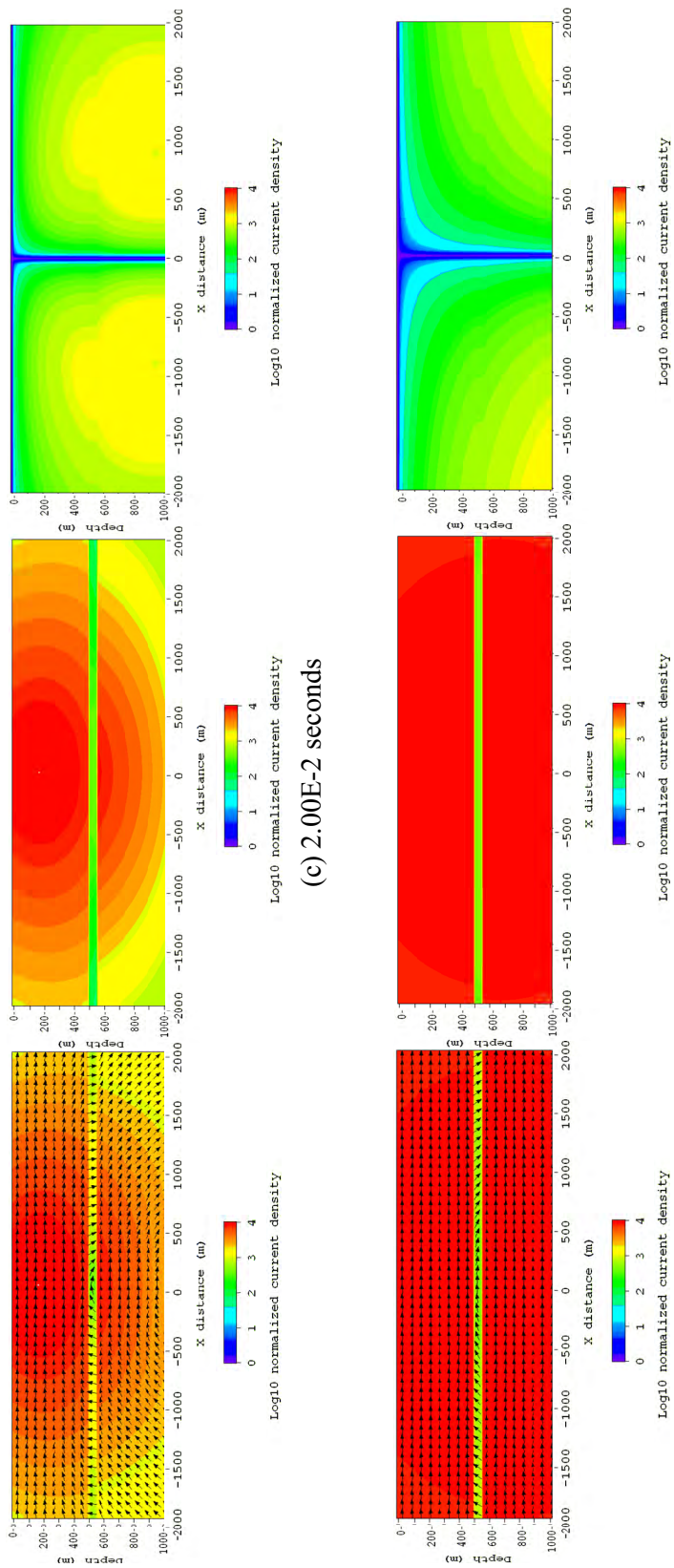

Figure 4.14. Continued.

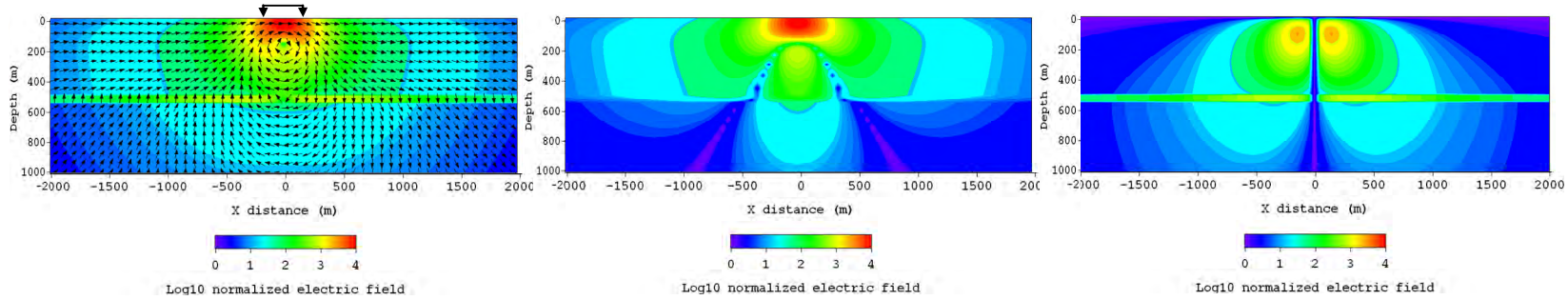

(a) 4.32E-4 seconds

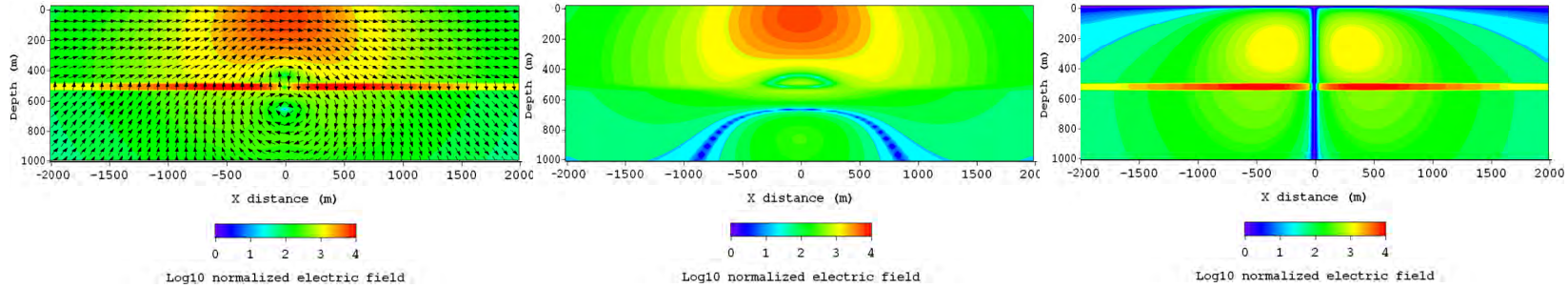

(b) 4.31E-3 seconds

Figure 4.15. Normalized electric field as a function of position in the cross-section including a 250 m long grounded source for the 1-D resistor model at the four different measurement times. Total electric field (left), horizontal electric field (middle) and vertical electric field (right).

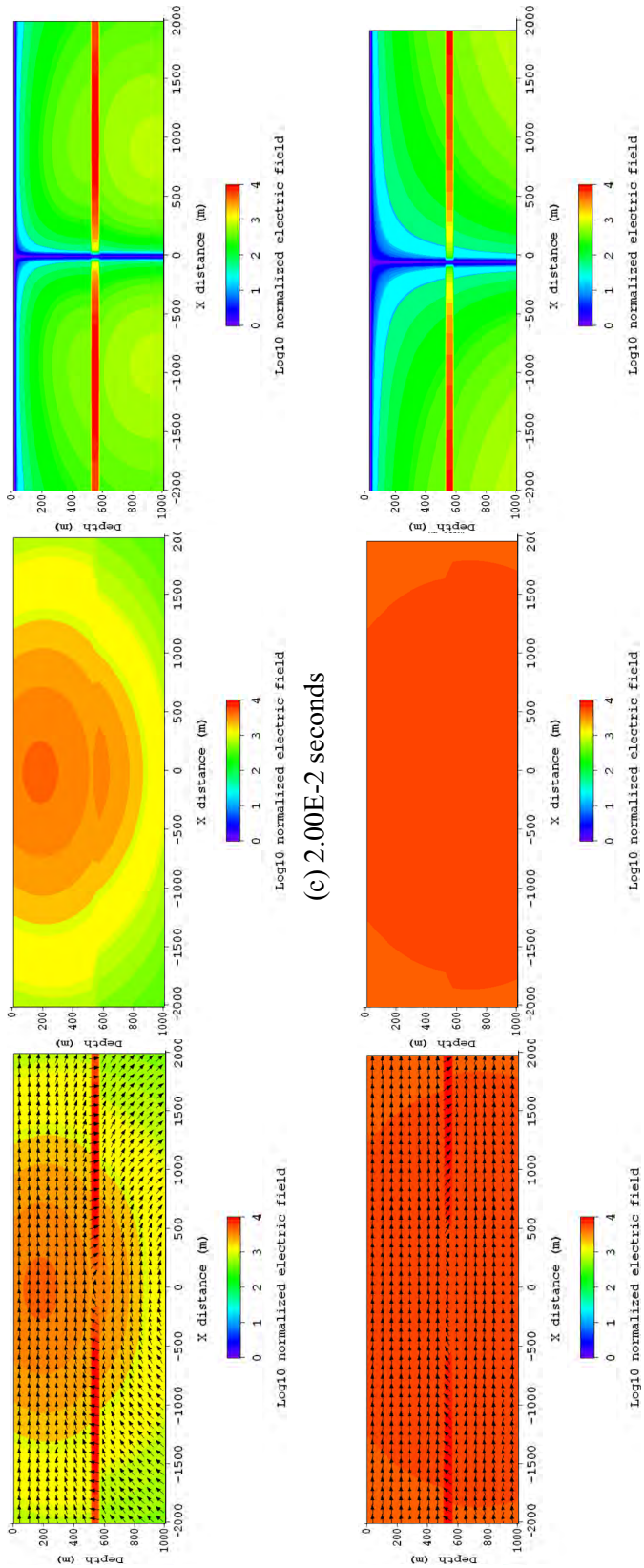

Figure 4.15. Continued.

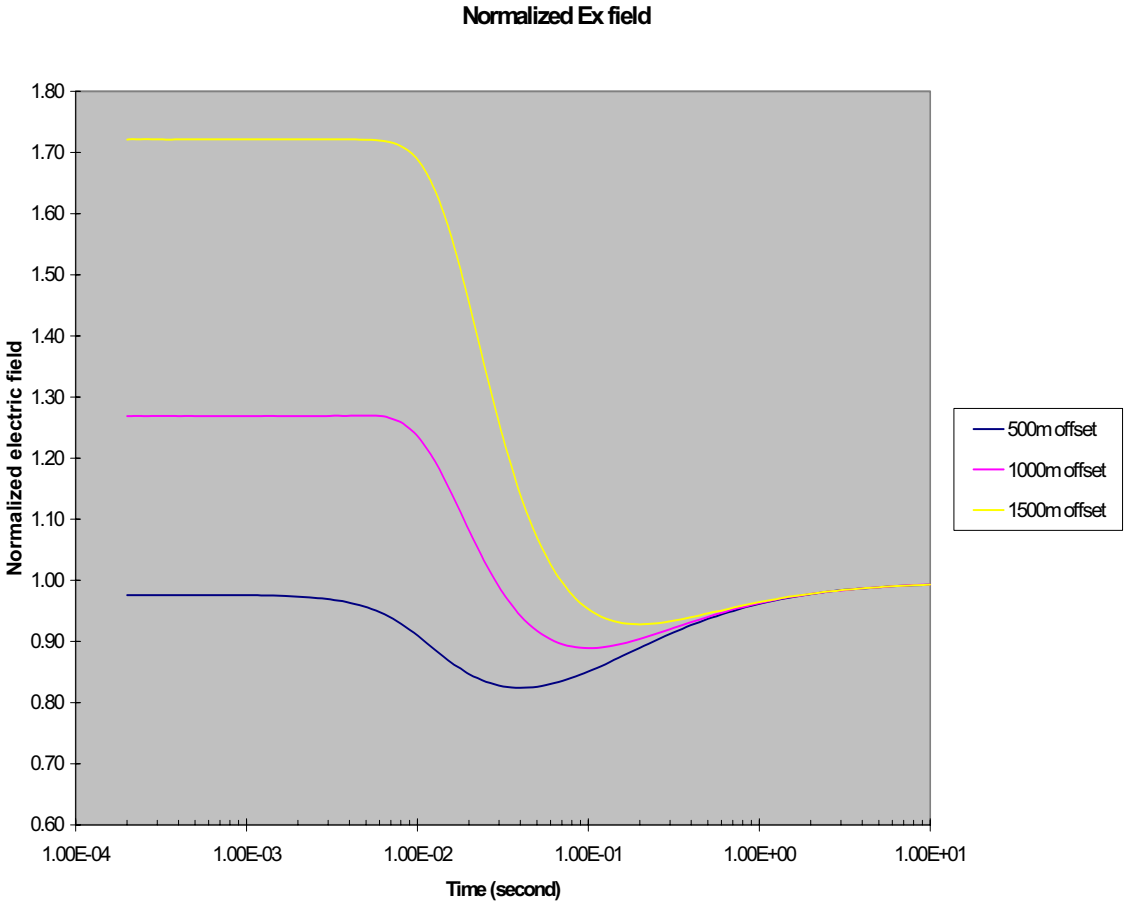

Figure 4.16. Normalized E_X fields for the 1-D resistor model at different source-receiver separations. Normalization is that of the background model.

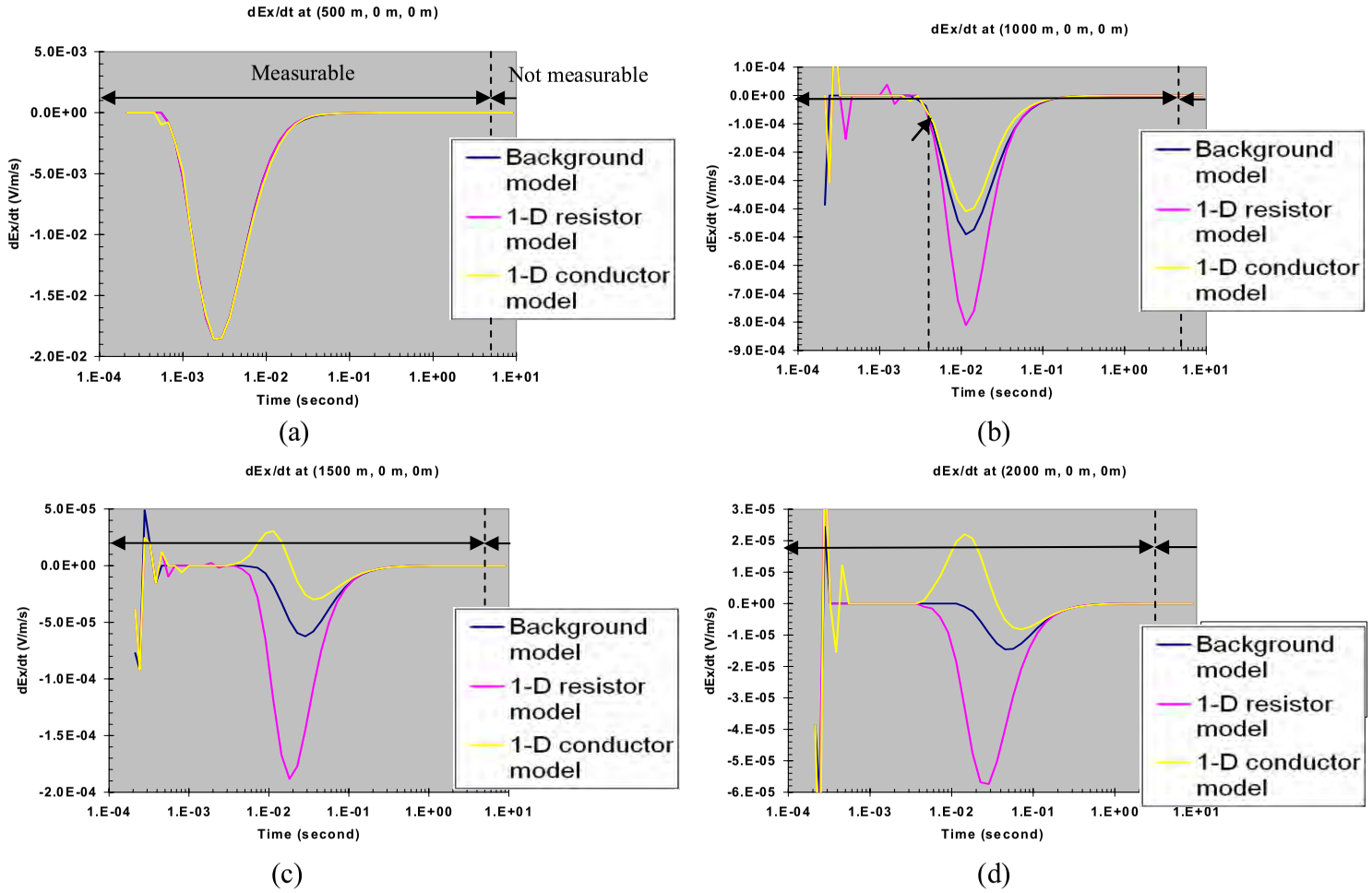

Figure 4.17. Time-derivatives of in-line GESTEM E_X response at different source-receiver separations. The arrow in (b) represents the time when the GESTEM method first starts to sense the presence of the thin conductor.

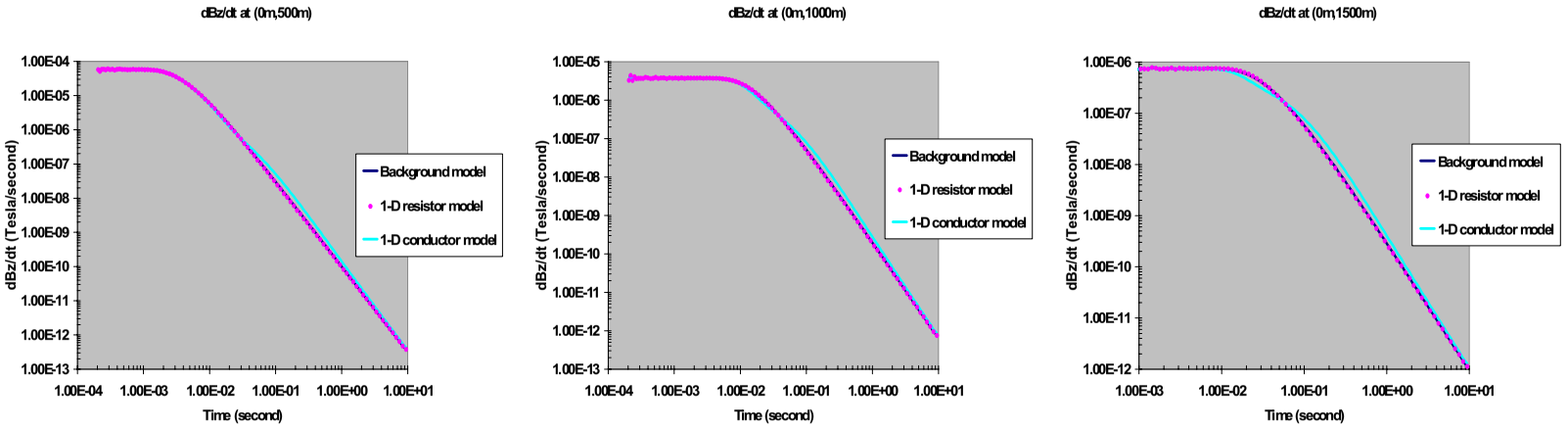

(a) (b) (c)

Figure 4.18. Broadside magnetic field response for a 250 m long grounded source.

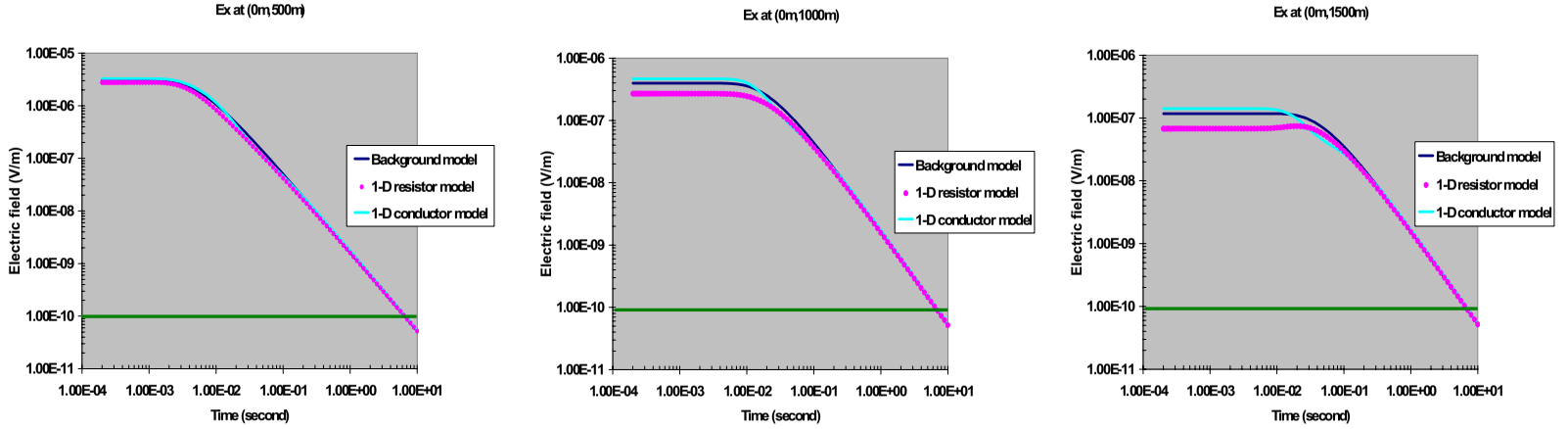

(a) (b) (c)

Figure 4.19. Broadside electric field response for a 250 m long grounded source. The green lines represent receiver noise level.

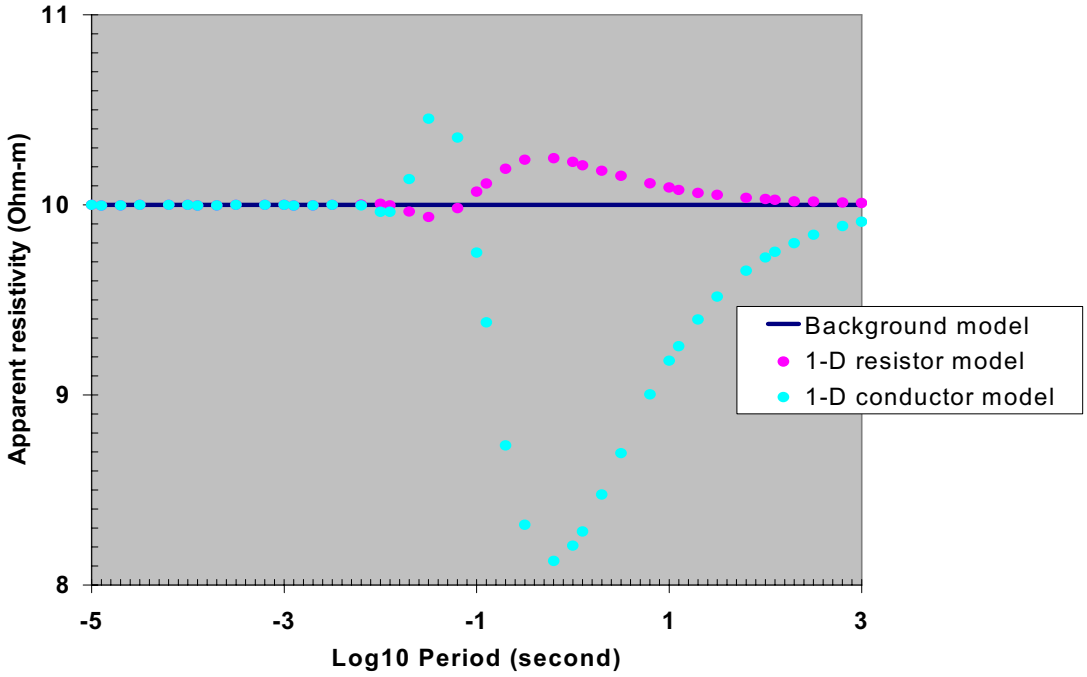

(a)

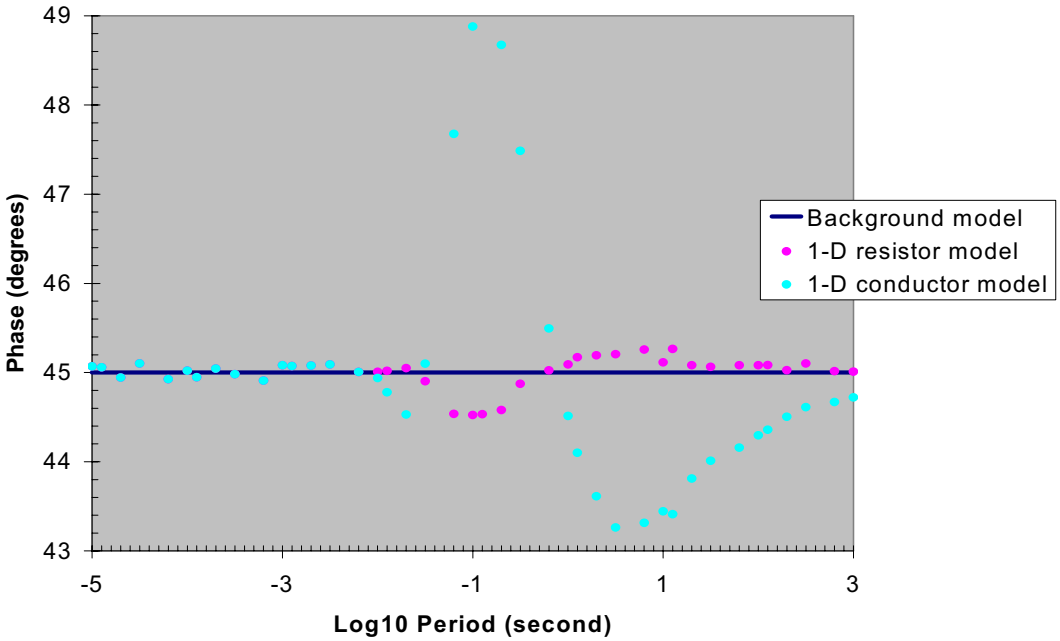

(b)

Figure 4.20. (a) AMT apparent resistivity curves and (b) impedance phase curves

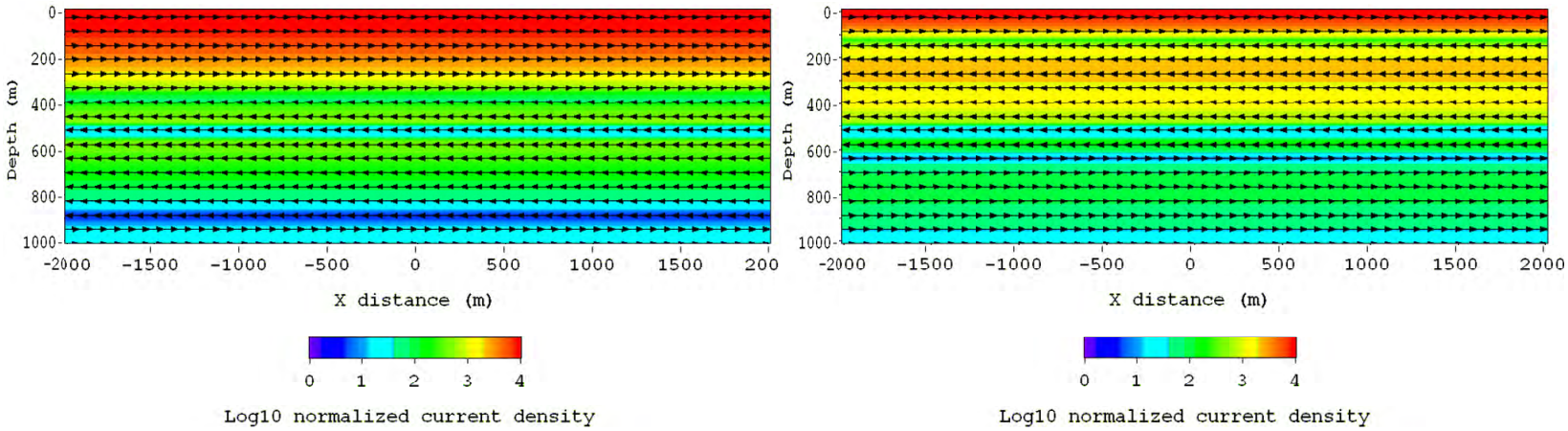

(a) In-phase

(b) Out-of-phase

Figure 4.21. Normalized in-phase and out-of-phase current density in the 1-D resistor model due to 100 Hz AMT plane wave source.

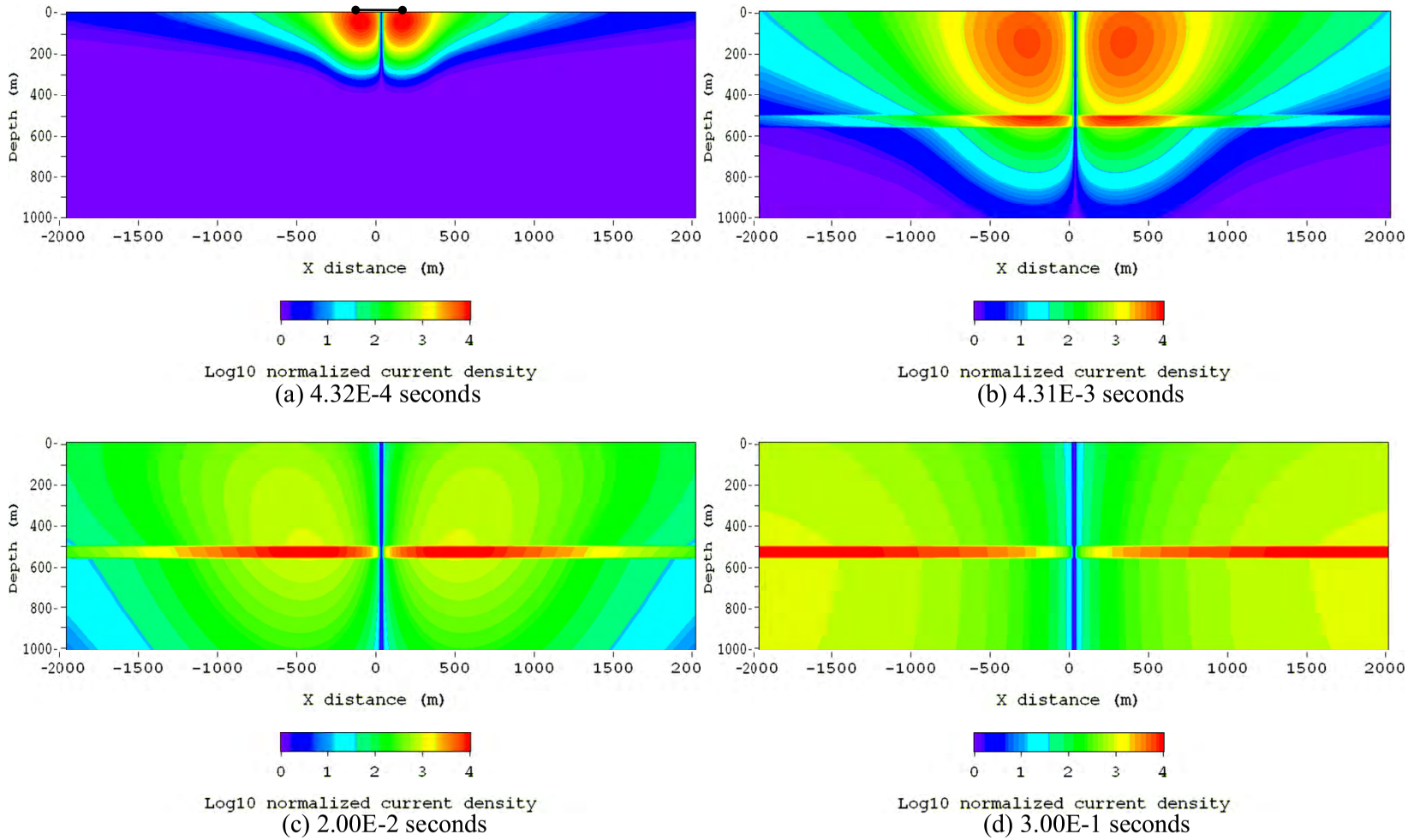

Figure 4.22. Normalized y component of the current density at the four different measurement times as a function of position in a plane bisecting a 250 m loop source in the 1-D conductor model.

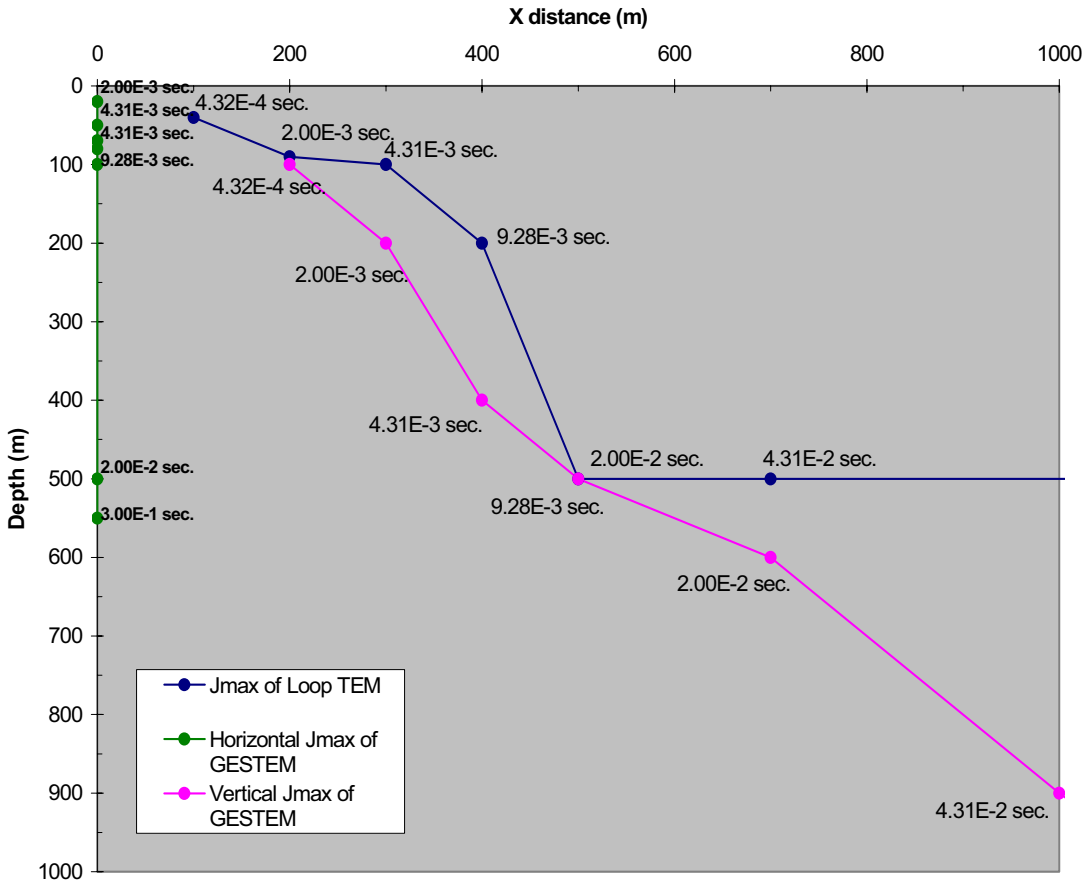

Figure 4.23. Locus of the current maximum in the 1-D conductor model.

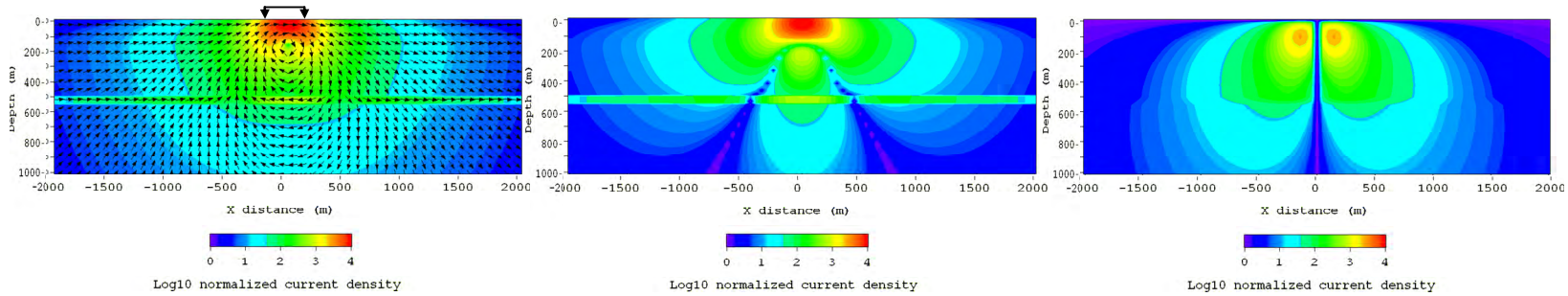

(a) 4.32E-4 seconds

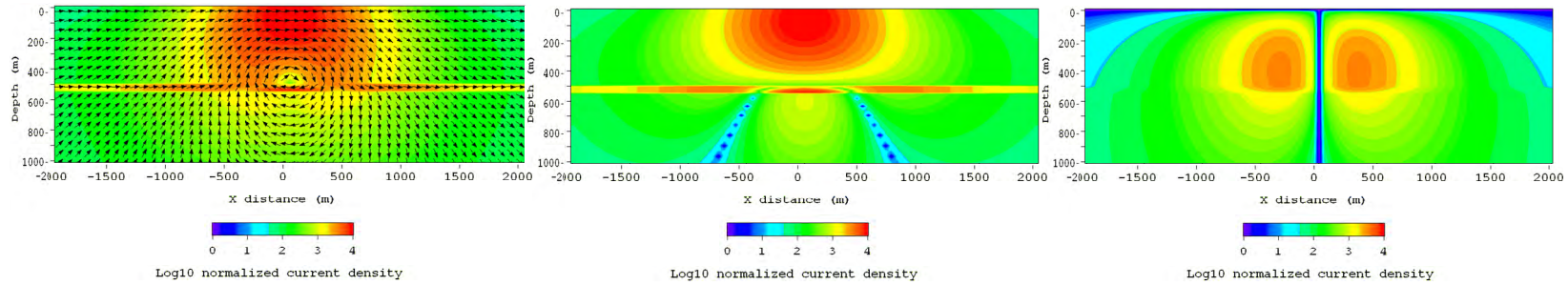

(b) 4.31E-3 seconds

Figure 4.24. Normalized current density as a function of position in the cross-section including a 250 m long grounded source for the 1-D conductor model at the four different measurement times. Total current density (left), horizontal current density (middle) and vertical current density (right).

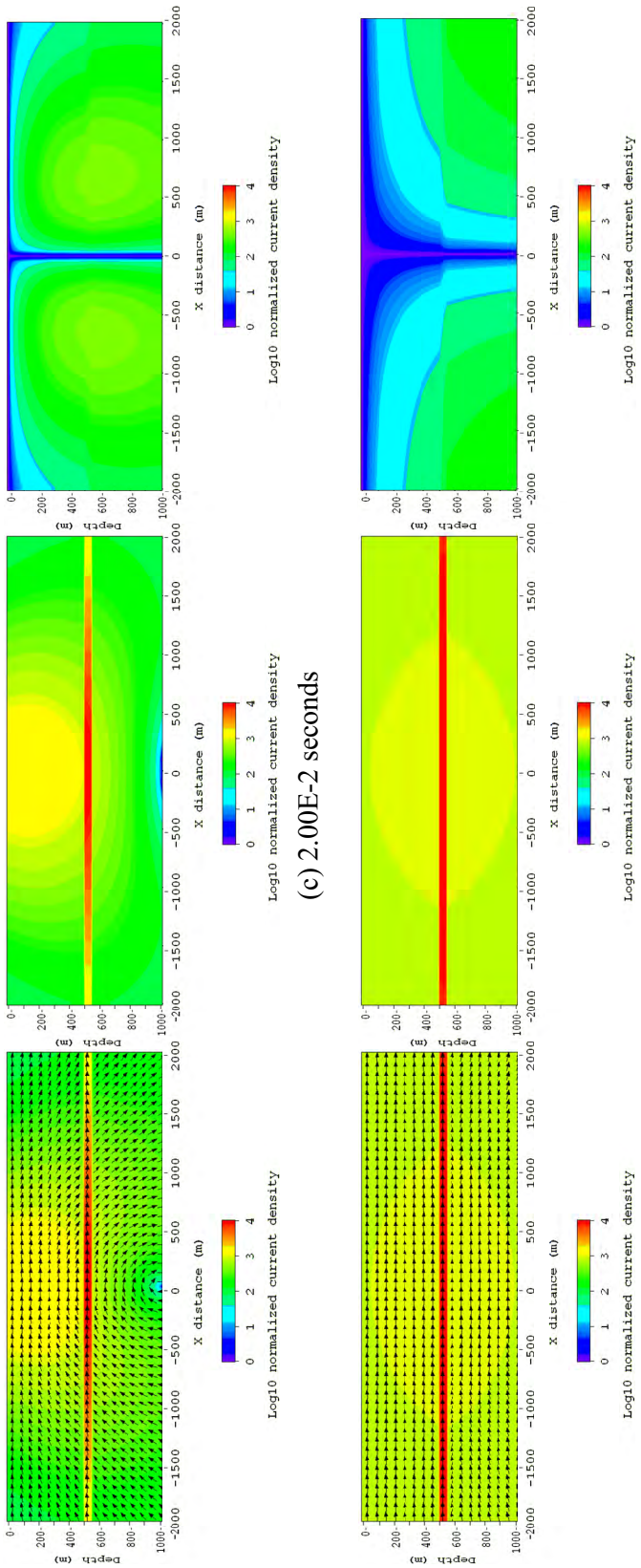

Figure 4.24. Continued.

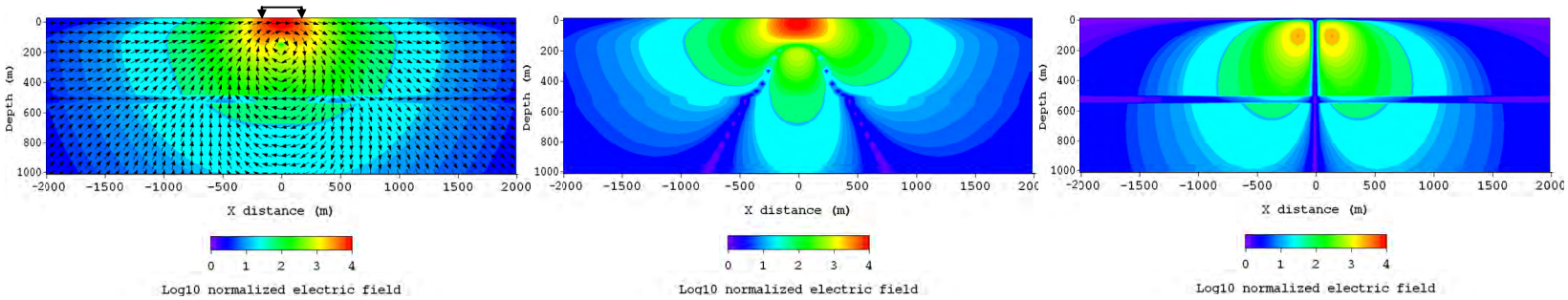

(a) 4.32E-4 seconds

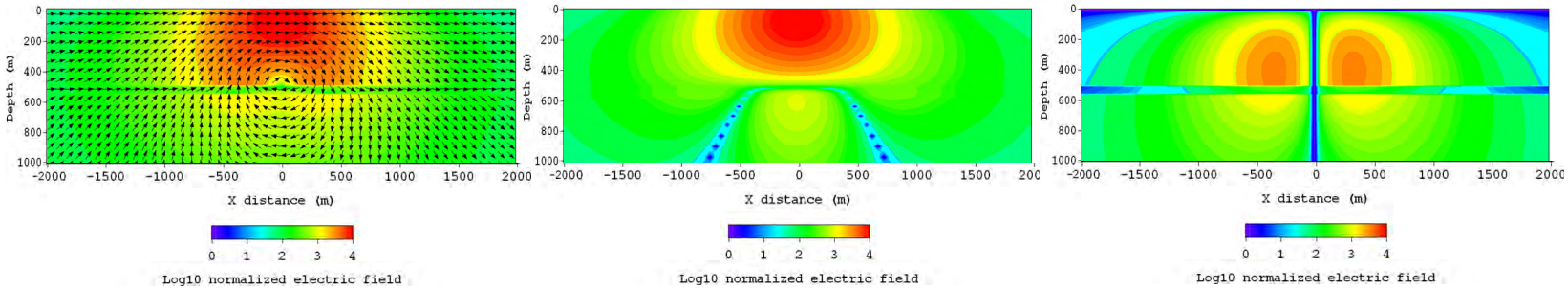

(b) 4.31E-3 seconds

Figure 4.25. Normalized electric field as a function of position in the cross-section including a 250 m long grounded source for the 1-D conductor model at four different measurement times. Total electric field (left), horizontal electric field (middle) and vertical electric field (right).

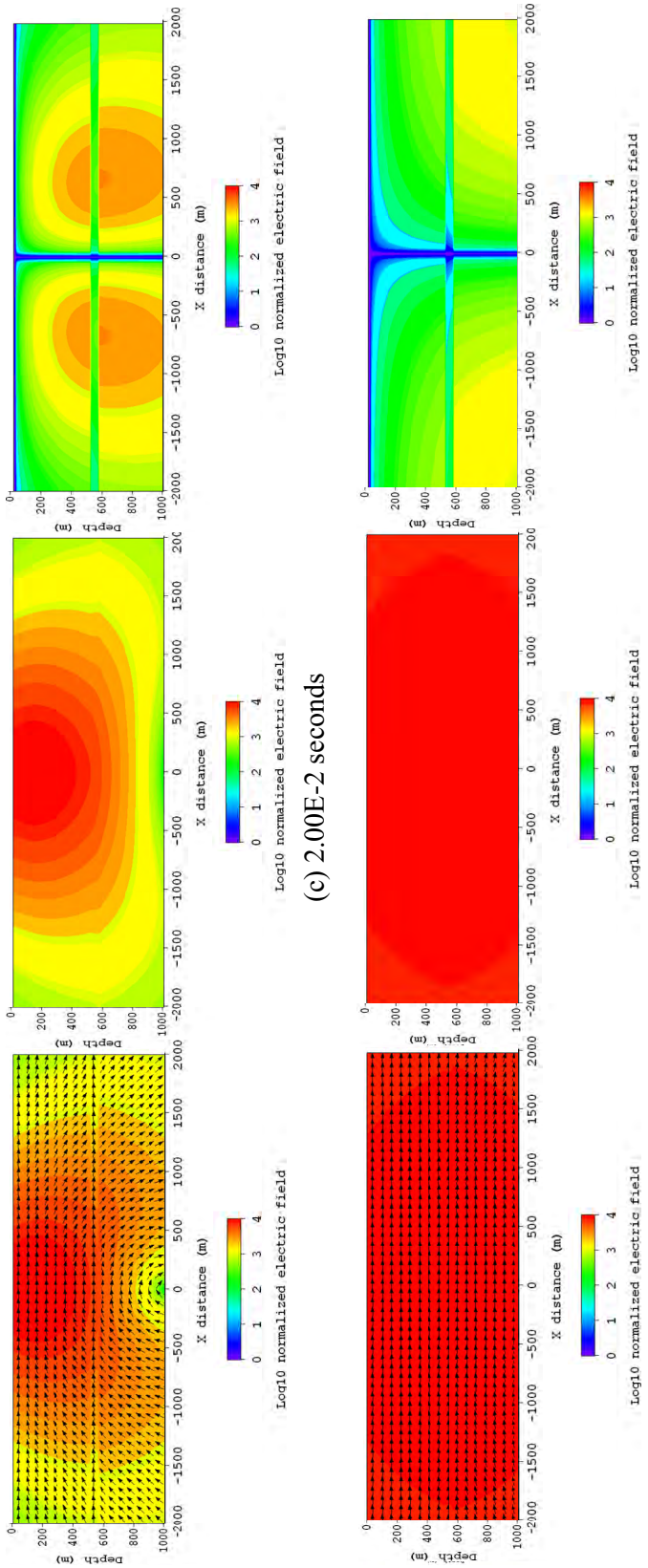

Figure 4.25. Continued.

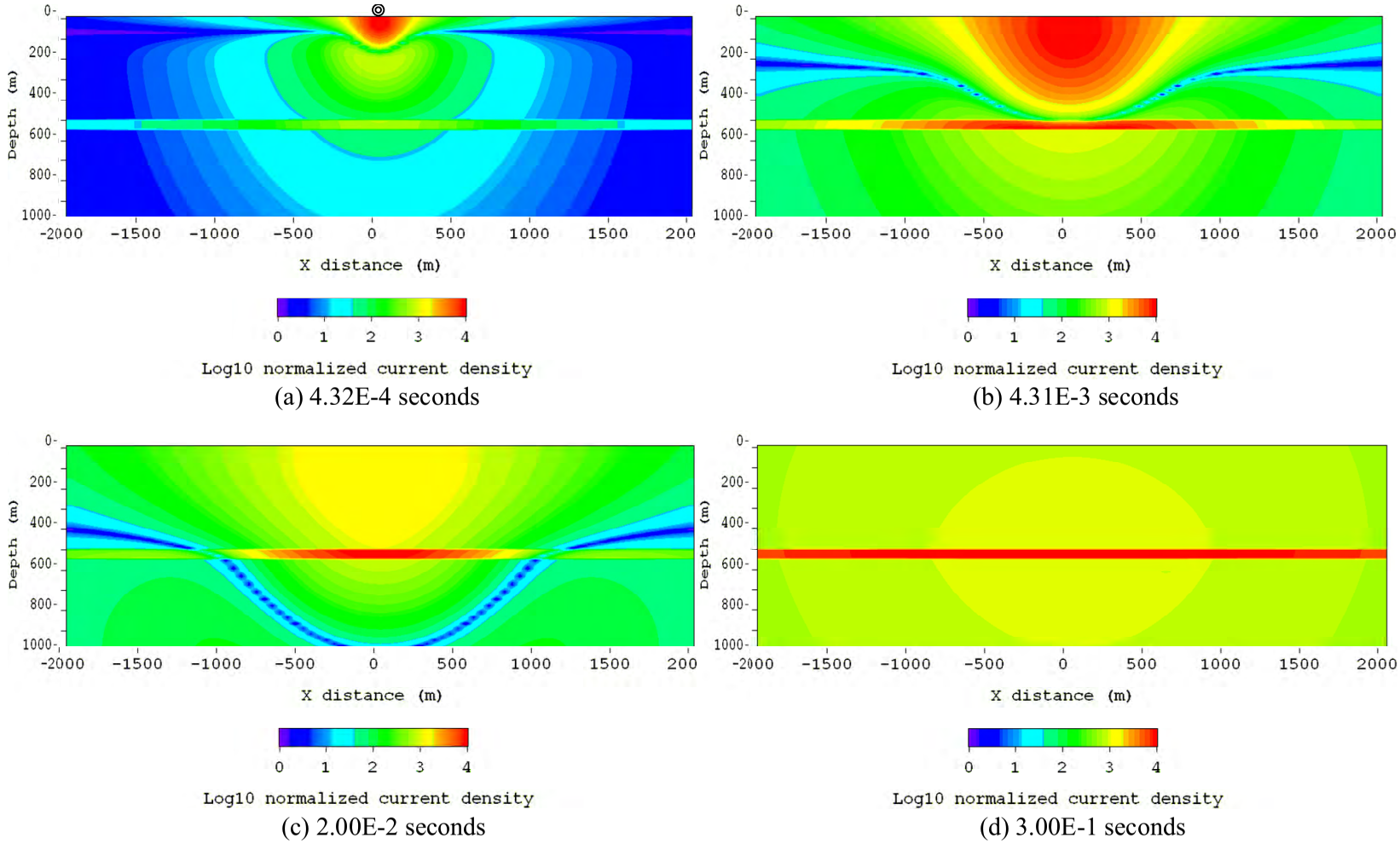

Figure 4.26. Normalized x component of the current density as a function of position in the cross-section bisecting a 250 m long grounded source for the 1-D conductor model at four different measurement times.

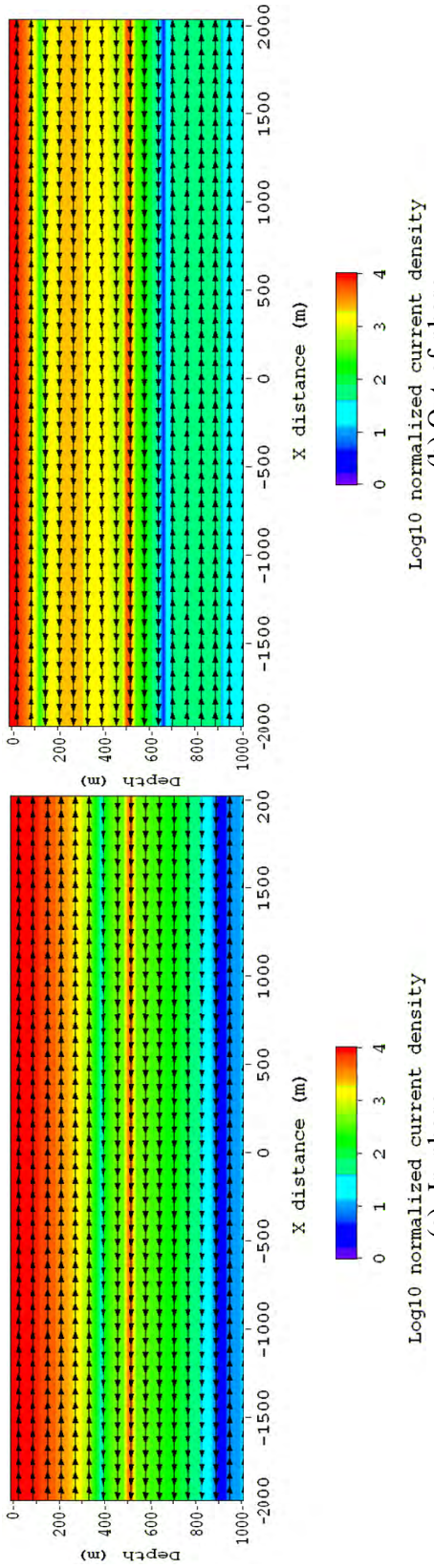

(a) In-phase (b) Out-of-phase

Figure 4.27. Normalized in-phase and out-of-phase current density in the 1-D conductor model due to 100 Hz AMT plane wave source.

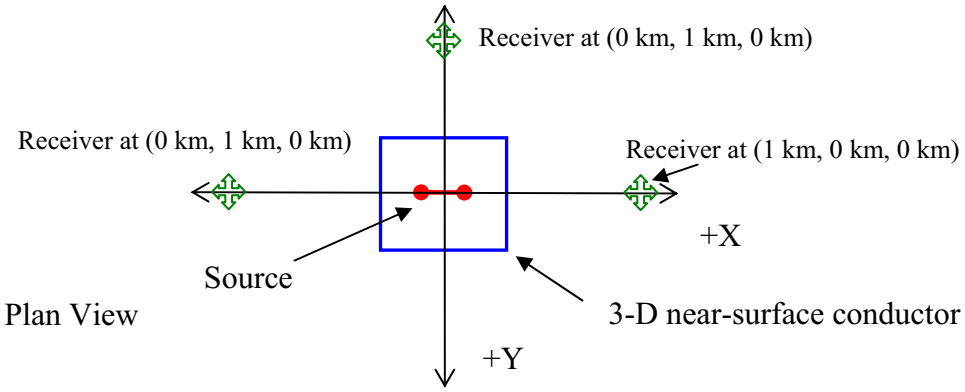

(a) Model 1: the center of the conductor at (0 m, 0m)

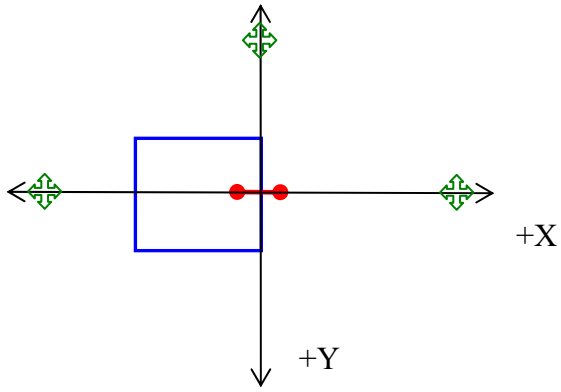

(b) Model 2: the center of the conductor at (-300 m, 0 m)

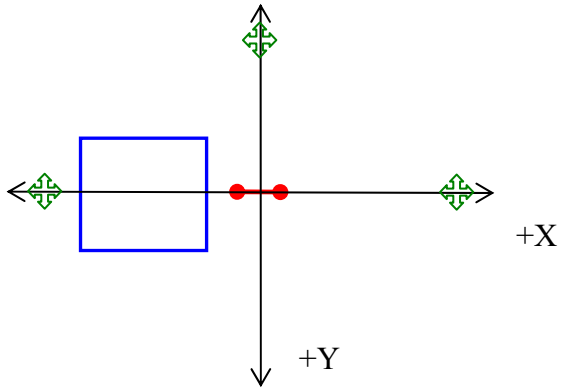

(c) Model 3: the center of the conductor at (-600 m, 0m)

Figure 4.28. The three near-surface inhomogeneity models. The center of the 250m long x-directed grounded source is placed at (0m, 0m, 0m). The dimension of the near-surface-conductor modeled as 1 Ohm-m is 600m(x)*600m(y) *100m(z) and the background is modeled as 10 Ohm-m.

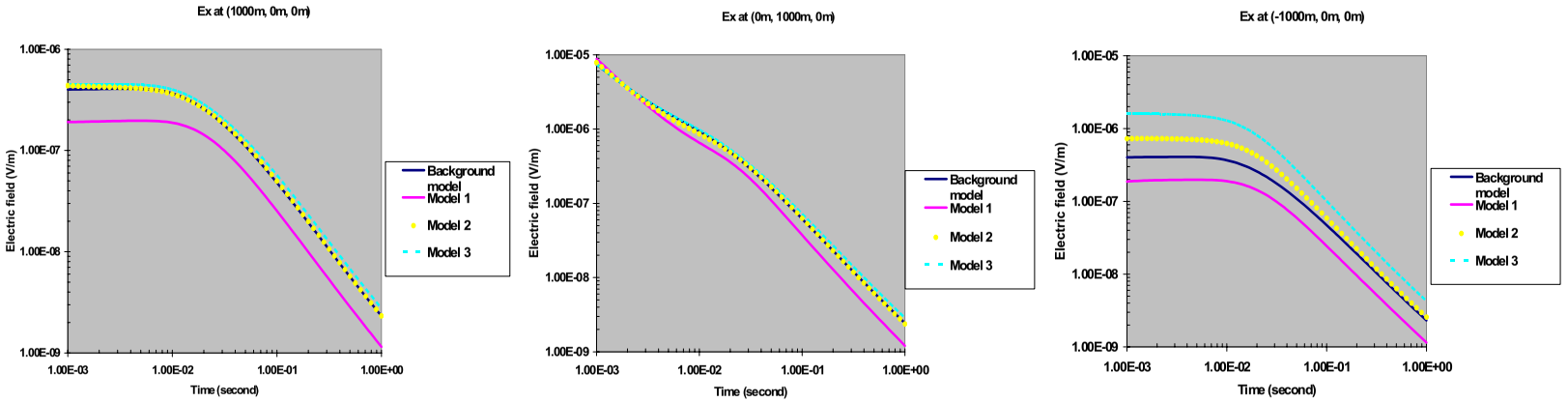

(a) (b) (c)

Figure 4.29. Transient electric field responses at the three different receiver locations for the three near-surface conductor models.

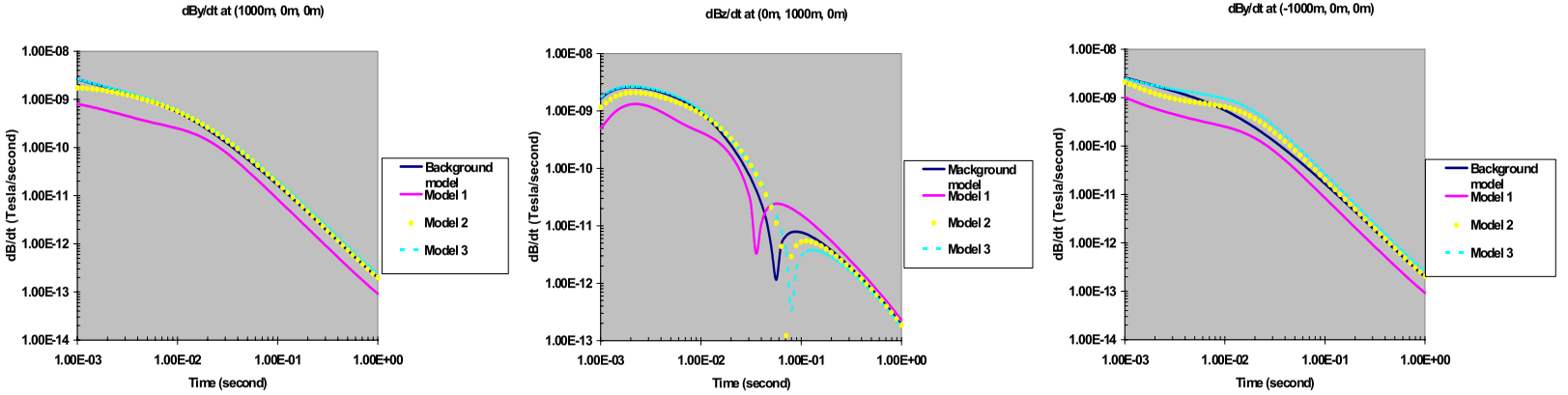

(a) (b) (c)

Figure 4.30. Transient magnetic field responses at the three different receiver locations for the three near-surface conductor models.

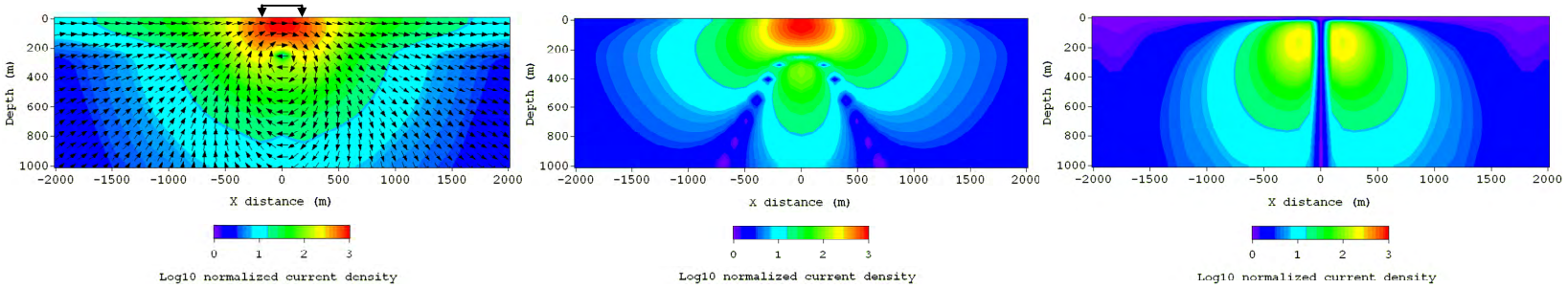

(a) 1.00E-3 seconds

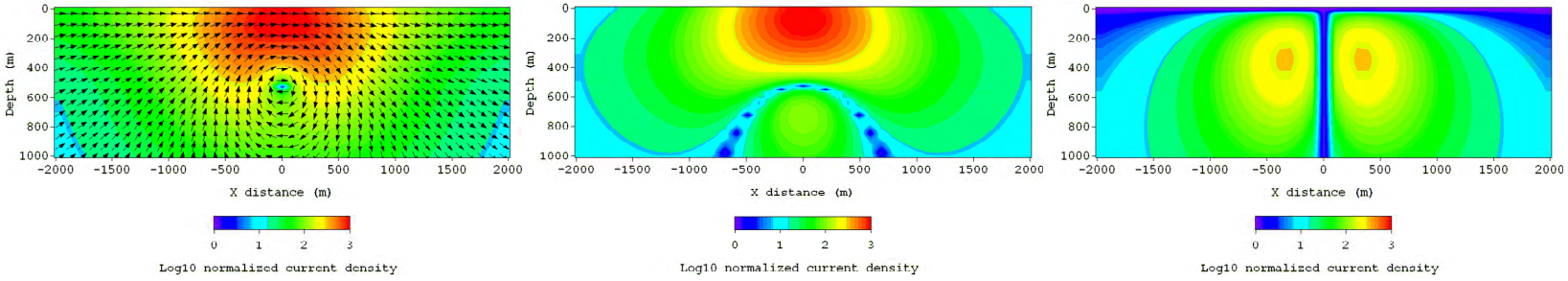

(b) 4.46E-3 seconds

Figure 4.31. Normalized current density as a function of position in the cross-section including a 250 m long grounded source for the background model at four different measurement times. Total current density (left), horizontal current density (middle) and vertical current density (right).

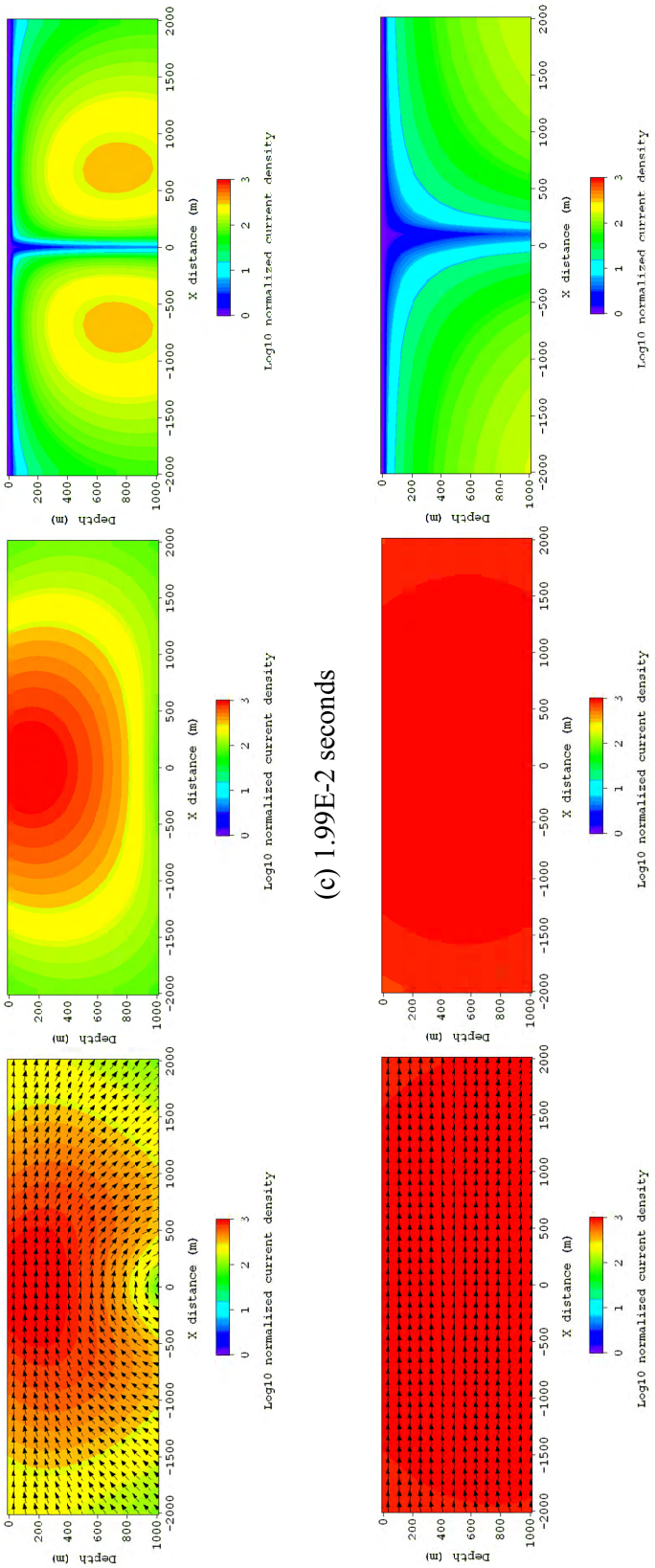

(c) 1.99E-2 seconds

(d) 0.32 seconds

Figure 4.31 Continued.

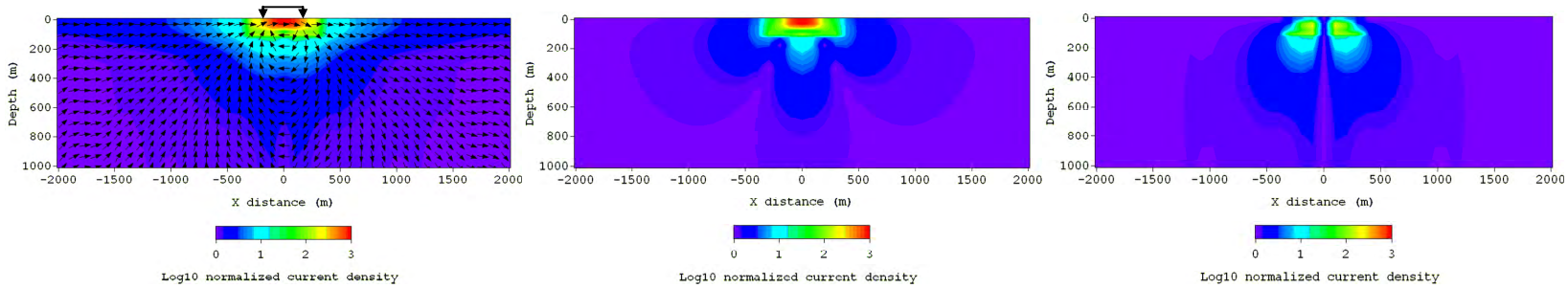

(a) 1.00E-3 seconds

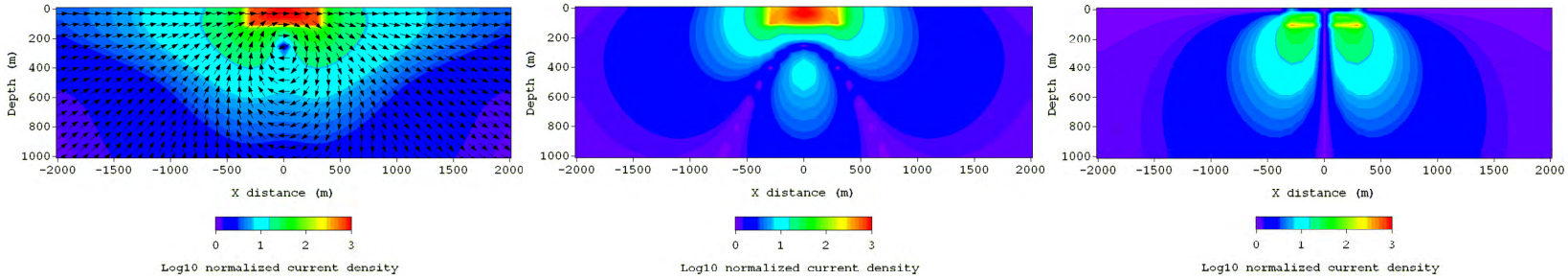

(b) 4.46E-3 seconds

Figure 4.32. Normalized current density as a function of position in the cross-section including a 250 m long grounded source for model 1 at four different measurement times. Total current density (left), horizontal current density (middle) and vertical current density (right).

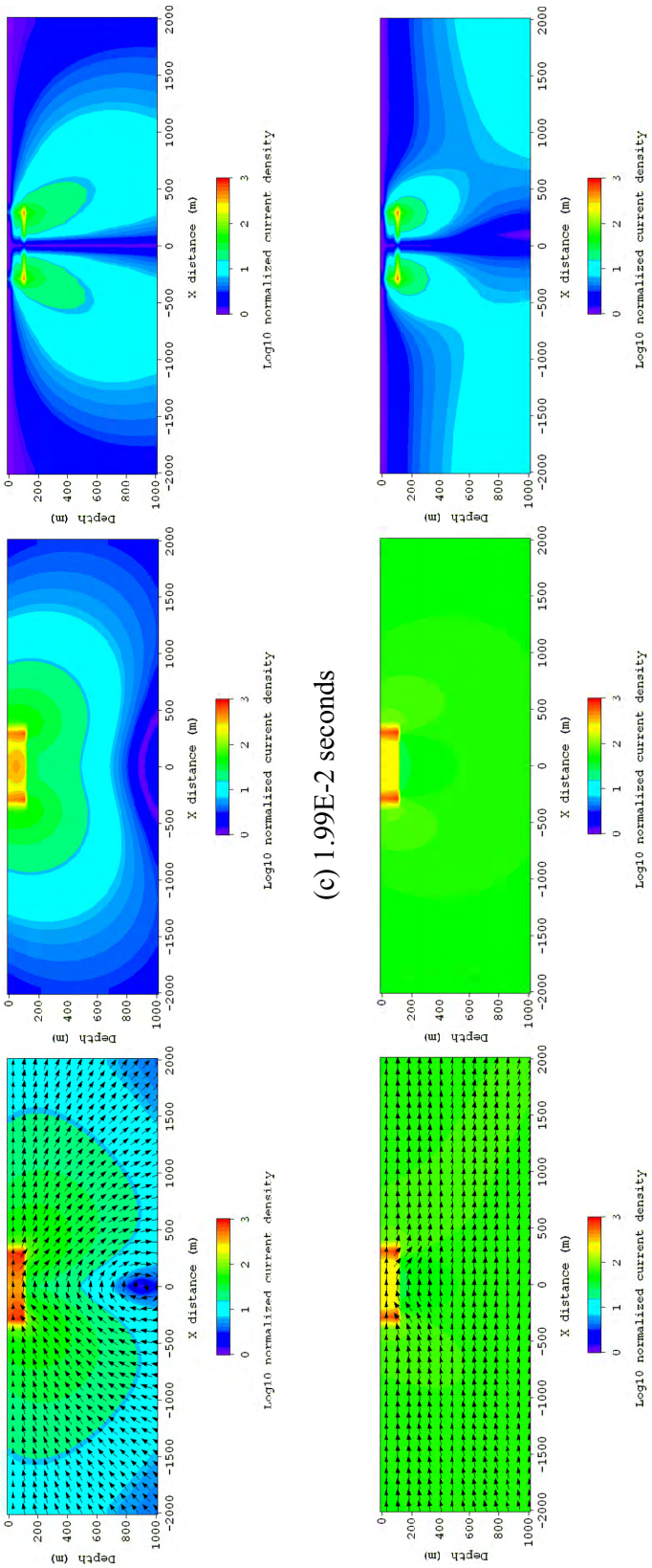

(c) 1.99E-2 seconds

(d) 0.32 seconds

Figure 4.32 Continued.

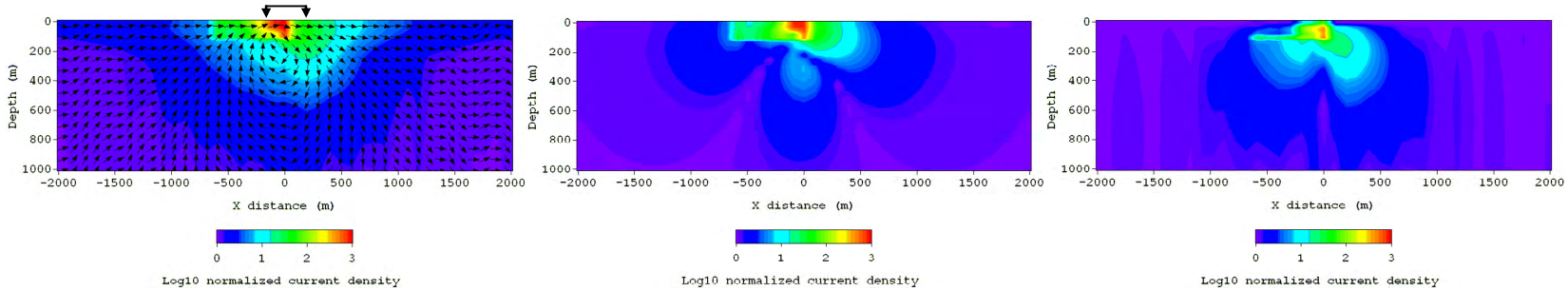

(a) 1.00E-3 seconds

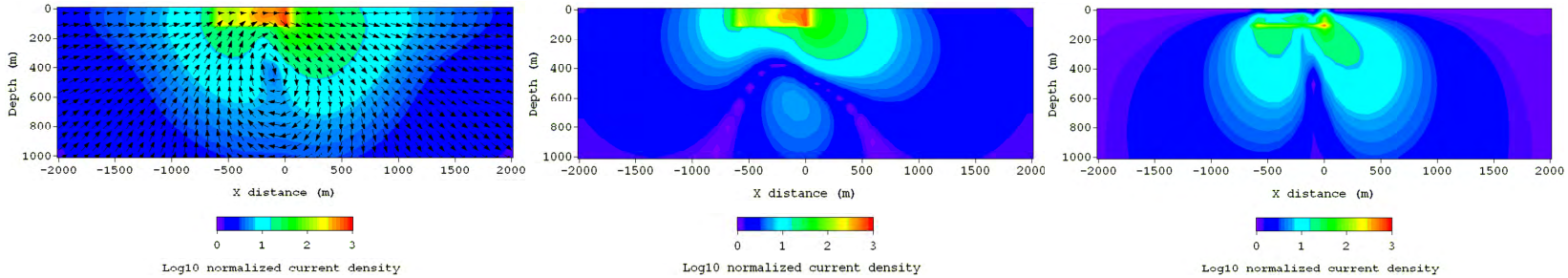

(b) 4.46E-3 seconds

Figure 4.33. Normalized current density as a function of position in the cross-section including a 250 m long grounded source for model 2 at four different measurement times. Total current density (left), horizontal current density (middle) and vertical current density (right).

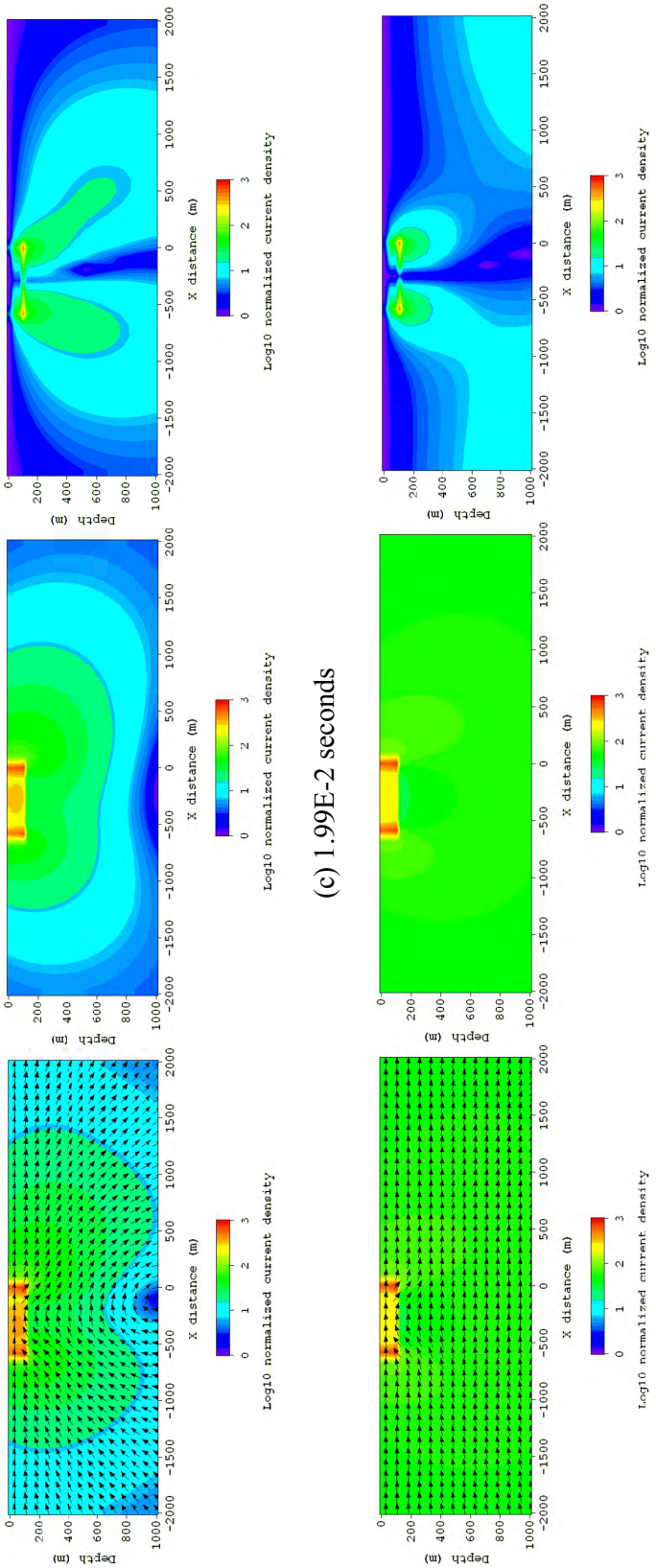

(c) 1.99E-2 seconds

(d) 0.32 seconds

Figure 4.33. Continued.

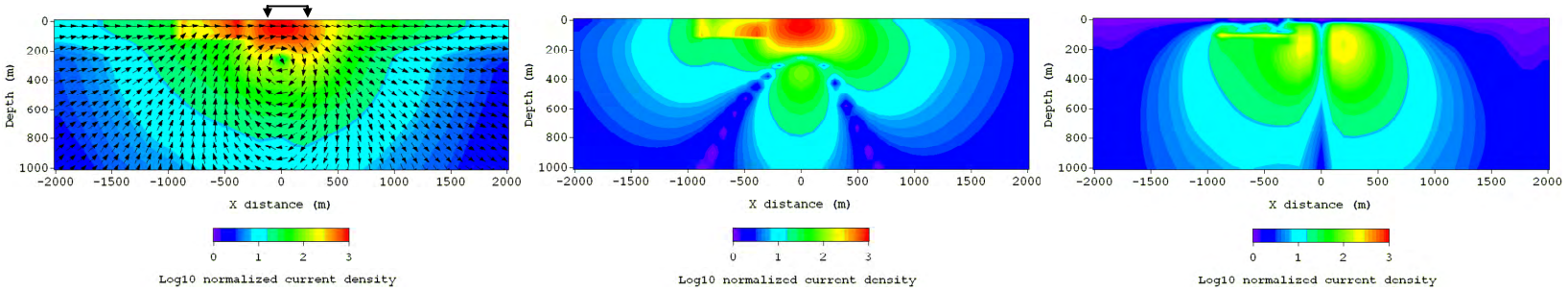

(a) 1.00E-3 seconds

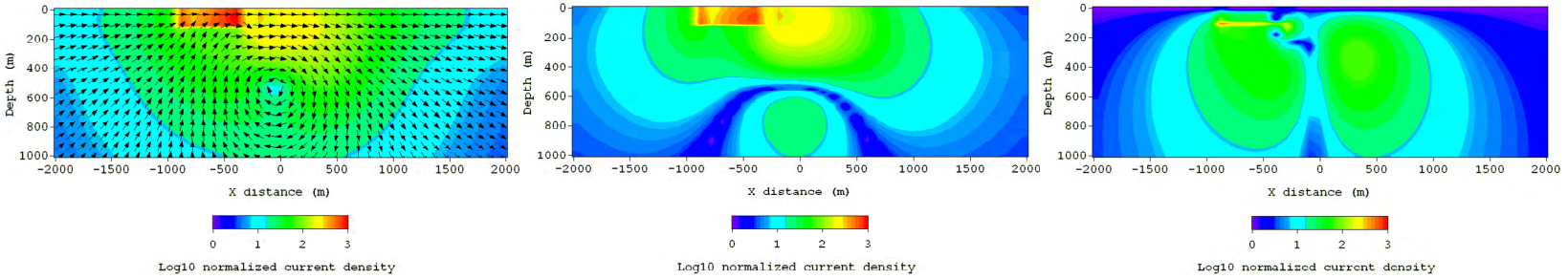

(b) 4.46E-3 seconds

Figure 4.34. Normalized current density as a function of position in the cross-section including a 250 m grounded source for model 3 at four different measurement times. Total current density (left), horizontal current density (middle) and vertical current density (right).

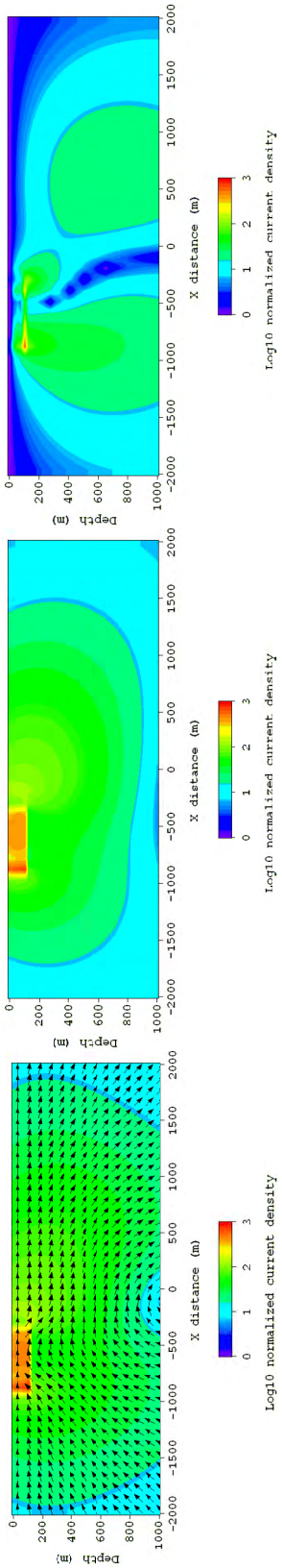

(c) 1.99E-2 seconds

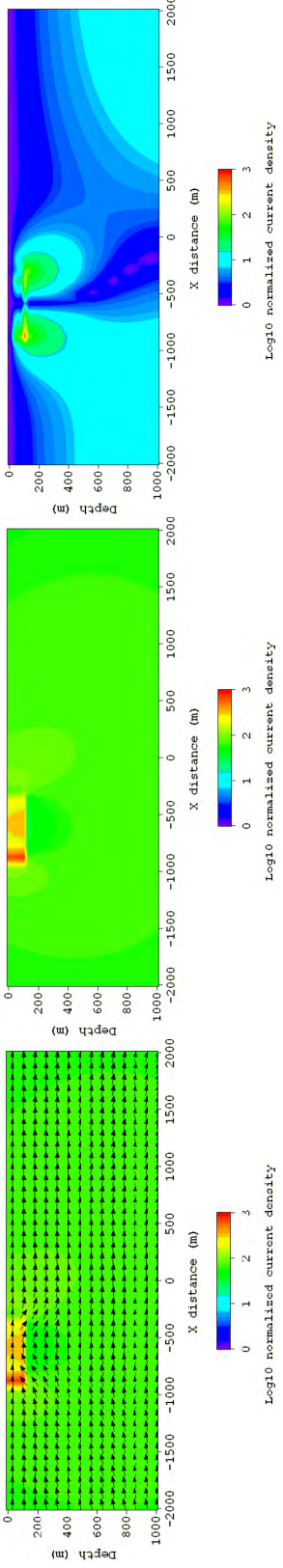

(d) 0.32 seconds

Figure 4.34. Continued.

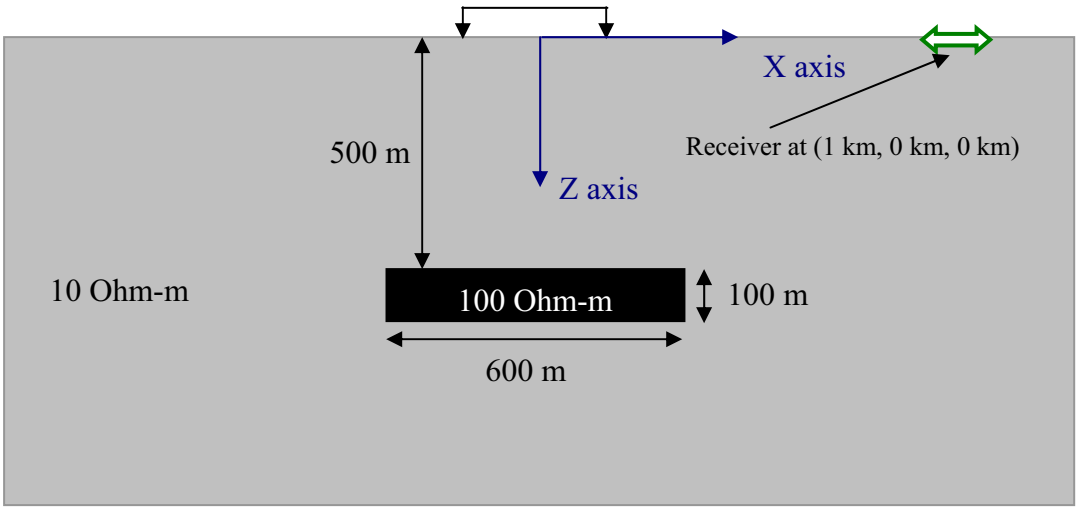

(a) Model 4

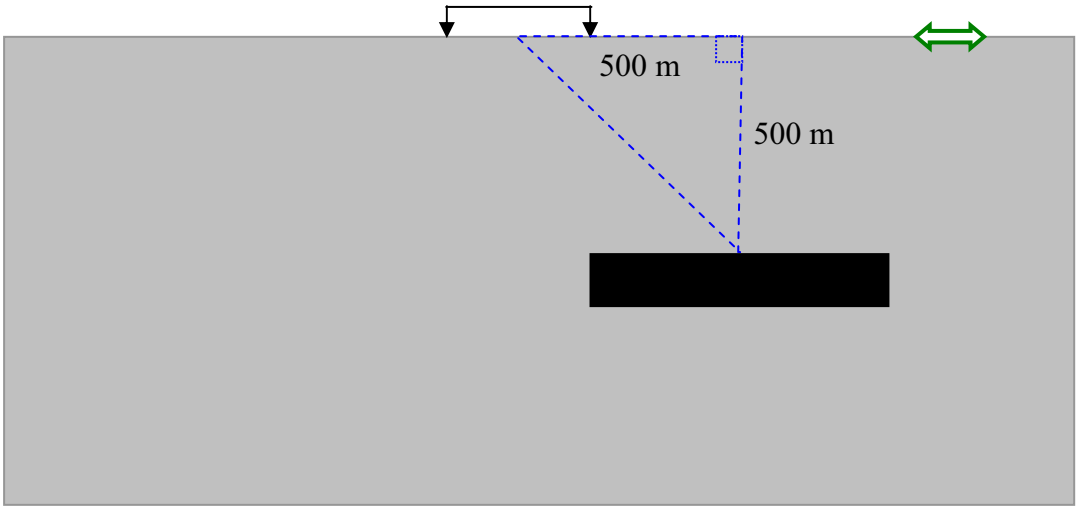

(b) Model 5

Figure 4.35. The 3-D resistive block models. (a) Model 4: the block is 500m below the center of the grounded source and (b) Model 5: the center of the block is moved 500m away from the center of the grounded source.

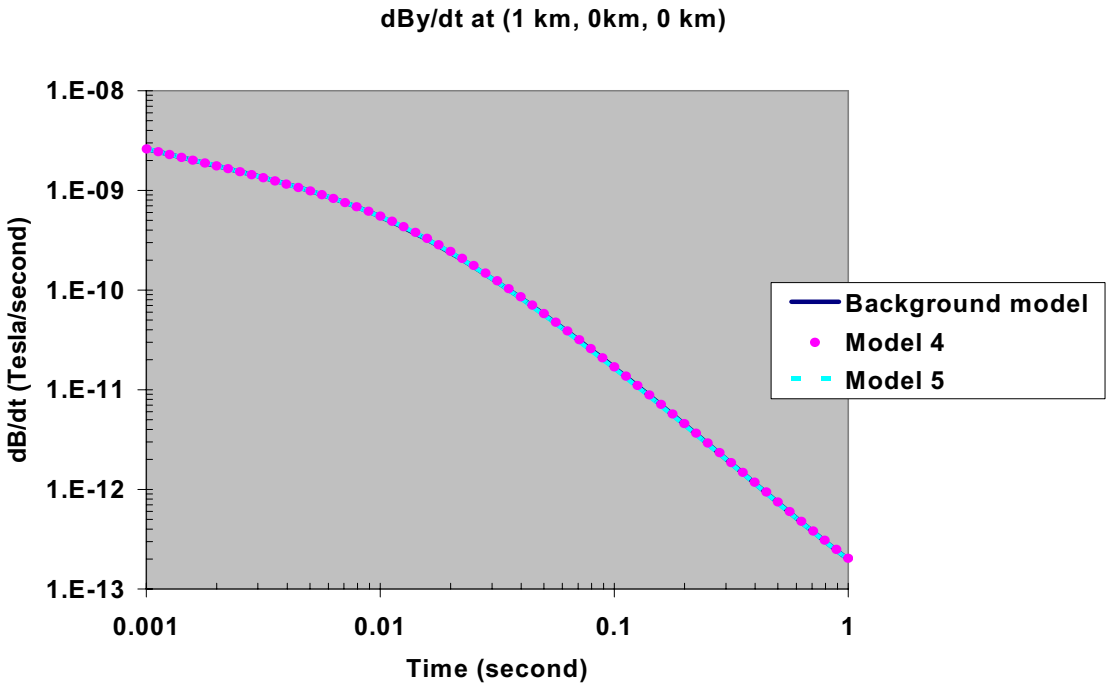

(a)

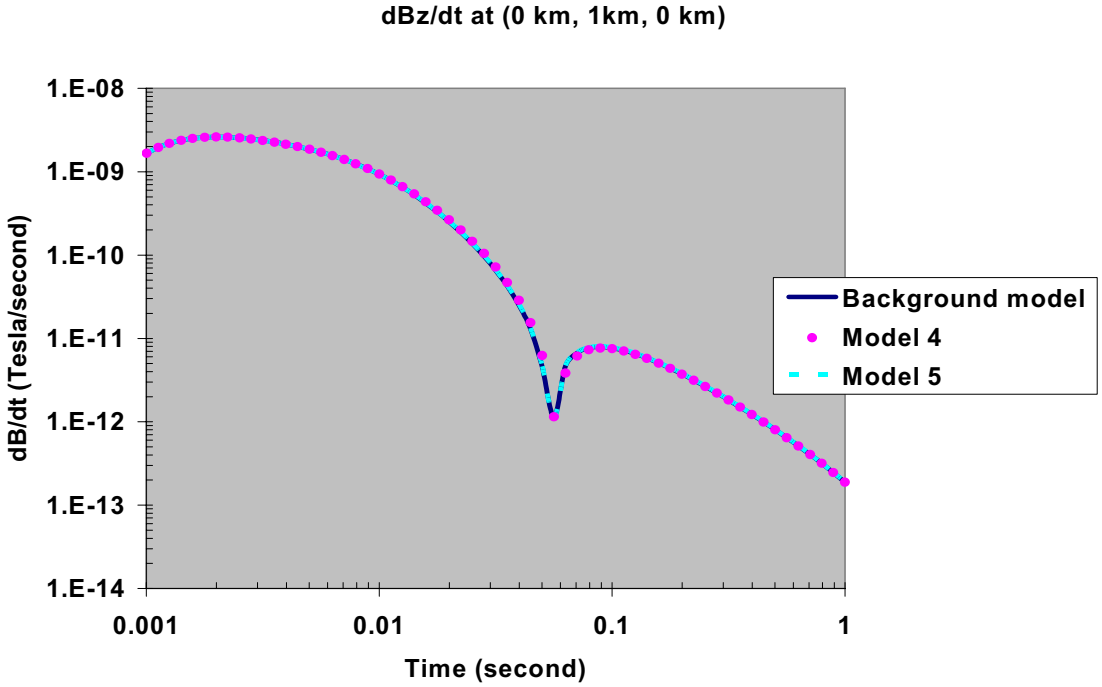

(b)

Figure 4.36. The magnetic field responses at the two receiver locations for 3-D resistive block models.

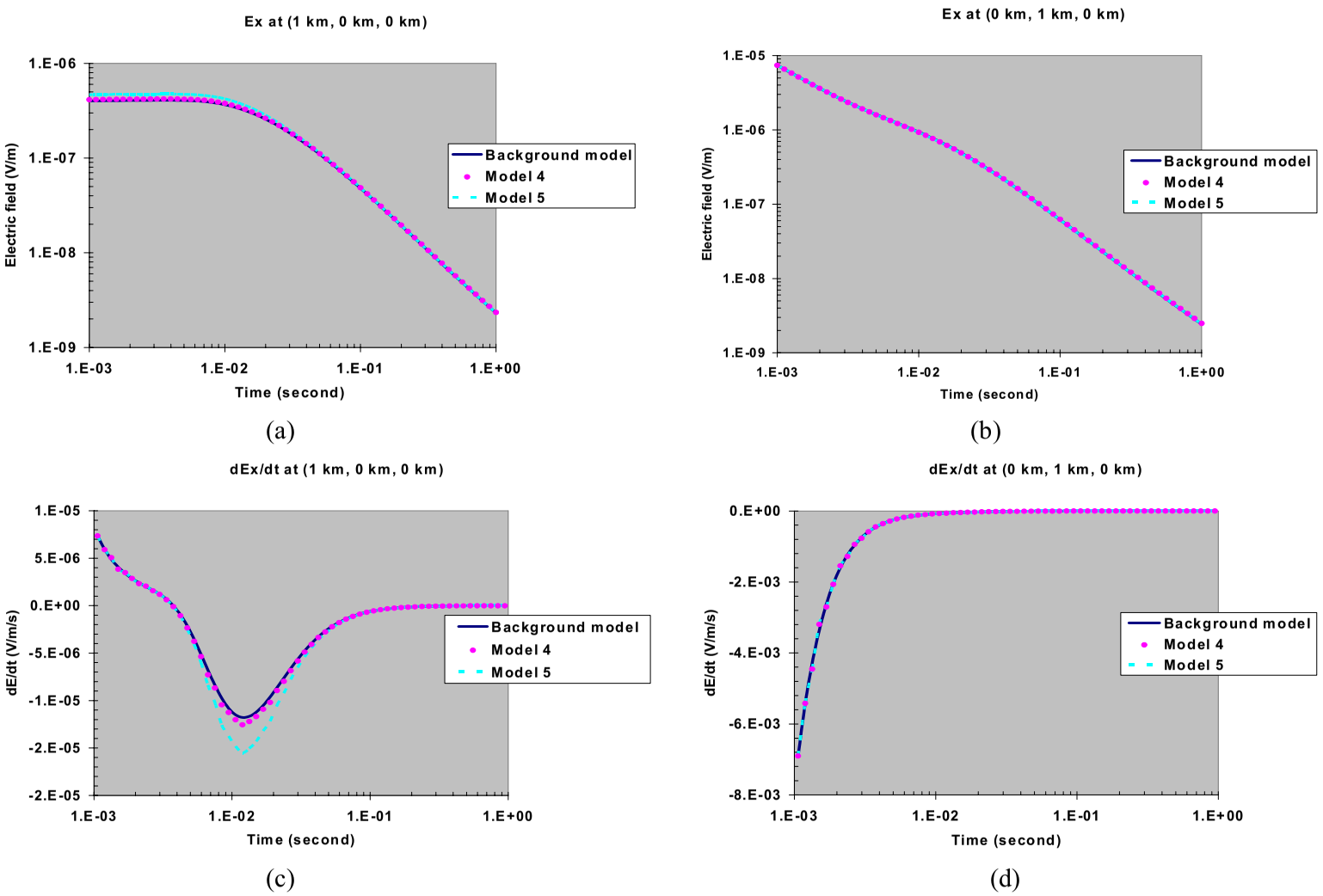

Figure 4.37. The electric field responses and their time-derivatives at the two receiver locations for 3-D resistive block models.

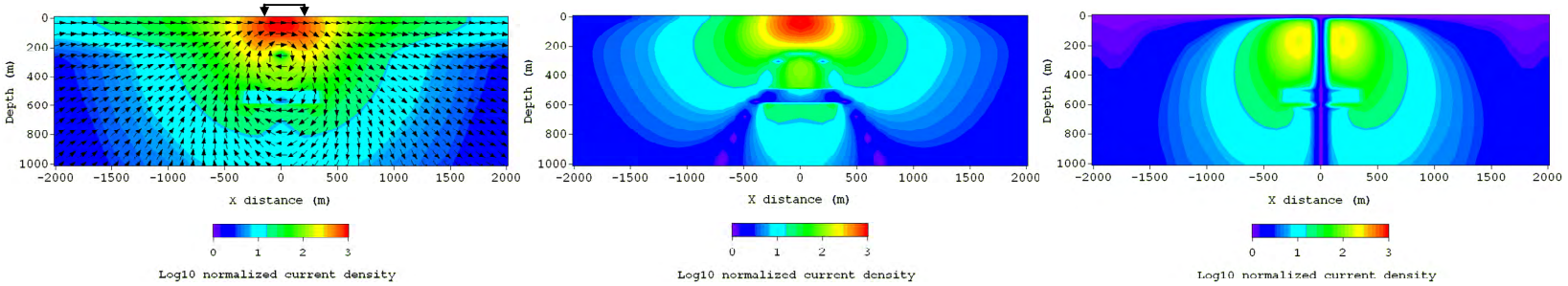

(a) 1.00E-3 seconds

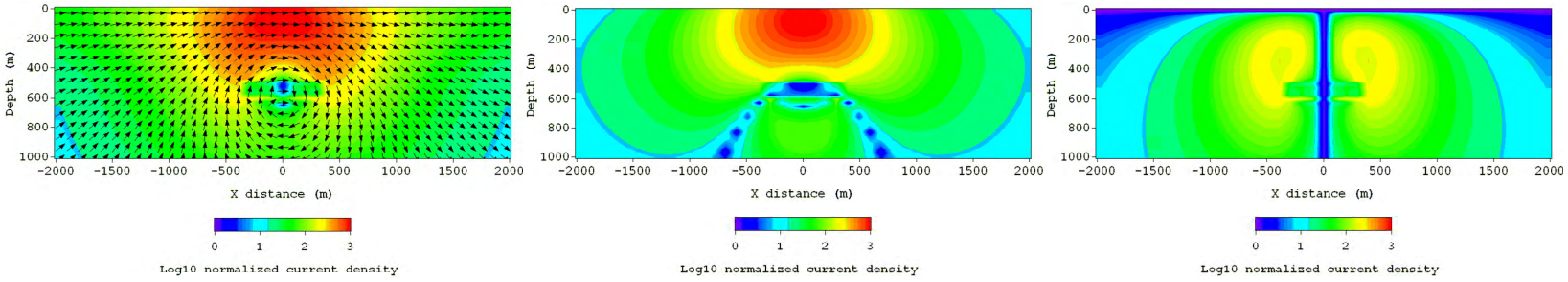

(b) 4.46E-3 seconds

Figure 4.38. Normalized current density as a function of position in the cross-section including a 250 m long grounded source for model 4 at four different measurement times. Total current density (left), horizontal current density (middle) and vertical current density (right).

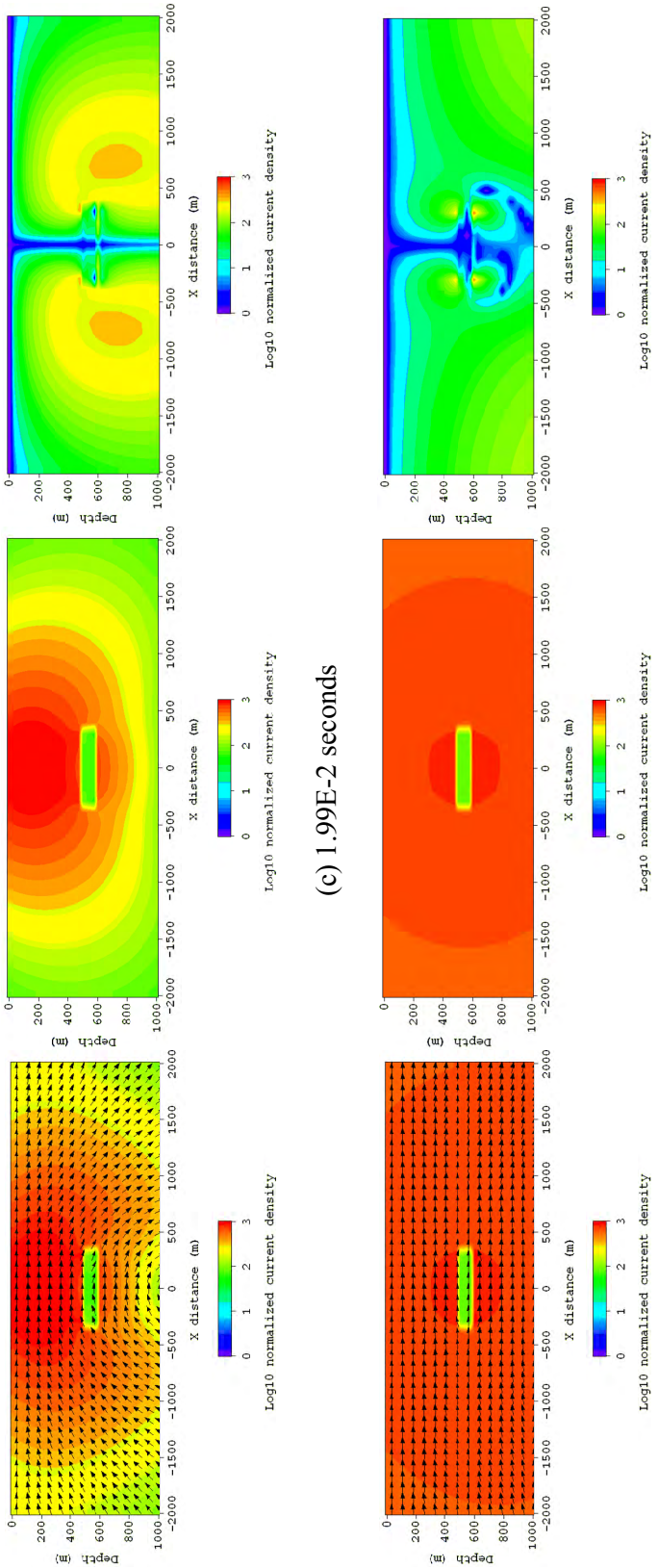

Figure 4.38. Continued.

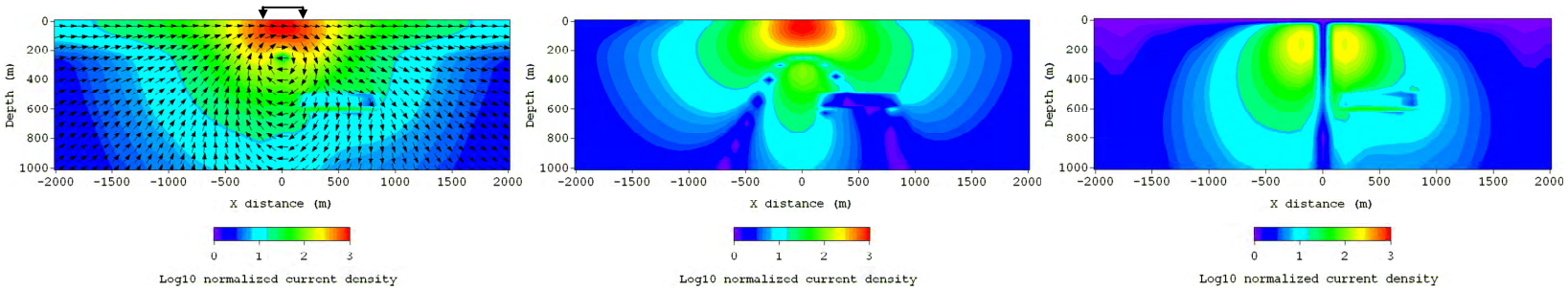

(a) 1.00E-3 seconds

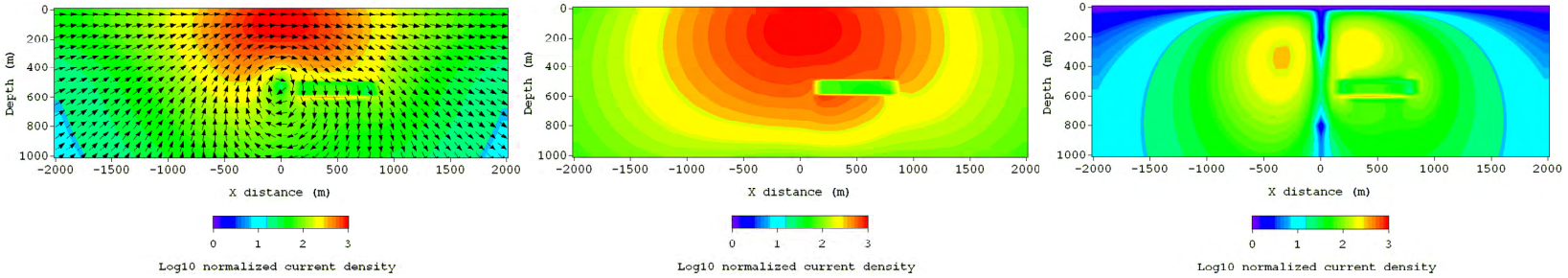

(b) 4.46E-3 seconds

Figure 4.39. Normalized current density as a function of position in the cross-section including a 250 m grounded source for model 5 at four different measurement times. Total current density (left), horizontal current density (middle) and vertical current density (right).

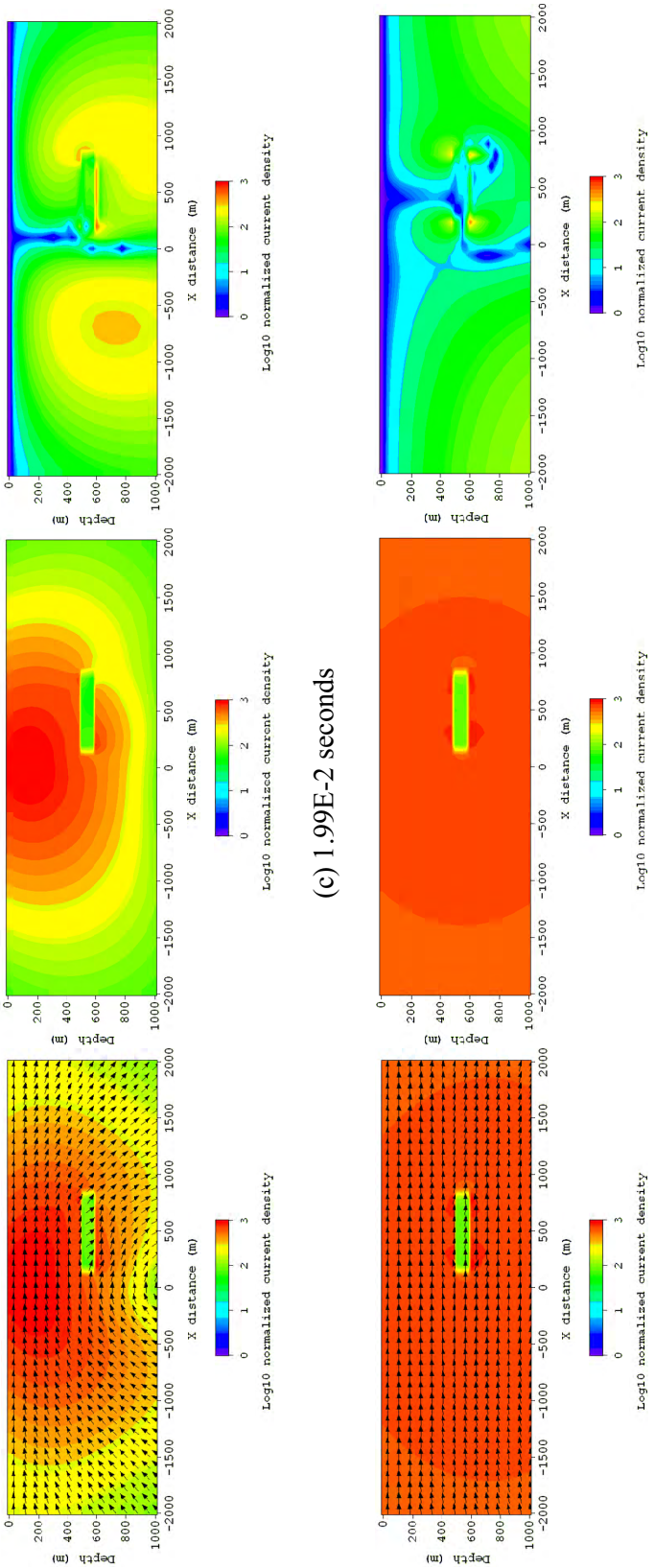

(c) 1.99E-2 seconds

(d) 0.32 seconds

Figure 4.39. Continued.